FERMI-LAB-PUB-75/52-T
COO-2220-52
June, 1975

Isospin $\frac{1}{2}$ Nucleon Resonance Production by a V, A Weak Neutral Current*

Stephen L. Adler
Fermi National Accelerator Laboratory, Batavia, Illinois 60510
and
The Institute for Advanced Study, Princeton, New Jersey 08540
and
Inga Karliner, Judy Lieberman, Yee Jack Ng and Hung-Sheng Tsao
The Institute for Advanced Study, Princeton, New Jersey 08540

ABSTRACT

We define a set of ratios characterizing the production of the isospin $\frac{1}{2}$ resonances $D_{13}(1514)$ and $S_{11}(1505)$, as well as the isospin 3/2 resonance $P_{33}(1232)$, by electromagnetic and weak (charged and neutral) currents. Assuming the most general weak neutral current with V, A spatial structure, we calculate the matrix elements needed to extract the production ratios in three dynamical models for resonance production: the Born approximation model, the nonrelativistic quark model and the quark bag model. For the special case of the Weinberg-Salam theory neutral current, the three models suggest that for $0 \leq \sin^2\theta_W \leq 0.5$ the ratios D_{13}/P_{33} and S_{11}/P_{33} observed in neutral current π^0 or η production on a free nucleon target should be substantially smaller (by a factor of 2 to 4) than the corresponding ratios observed in charged current π^0 or η production. We also attempt to predict the ratios D_{13}/P_{33} and S_{11}/P_{33} to be expected in charged current production from the corresponding ratios observed in electroproduction, but here the three models do not agree, and so we can only state a wide possible range in which the values of the ratios may lie. We briefly discuss the charge exchange corrections needed for comparison with experiments on complex nuclear targets; we find for an aluminum target that the reduction factors quoted above are halved, so that in neutral current induced reactions the ratios D_{13}/P_{33} and S_{11}/P_{33} are smaller by a factor of 1 to 2 than the corresponding ratios observed in charged current induced reactions.

---

* Research sponsored in part by the Atomic Energy Commission, Grant No. AT(11-1)-2220.

I. INTRODUCTION

Inelastic exclusive channels have an important role to play in studying the structure of the semileptonic weak neutral current. The most prominent such channel, and the one which has received the most theoretical[1,2] and experimental[3] attention so far, is pion production in the region of the I = 3/2 resonance $P_{33}(1232)$. We turn in the present paper to the study of what are expected to be the most prominent[4] I = 1/2 structures excited in neutral current experiments, the resonances $D_{13}(1514)$ and $S_{11}(1505)$. There are two principal reasons for interest in these states. First, in experiments with low invariant mass resolution, π^0's coming from decay of the I=1/2 states may bias invariant mass plots at the high side of the $P_{33}(1232)$; in order to understand this possible bias, estimates of the production of the I=1/2 states by the neutral current are needed.[5] Second, observation of the I=1/2 states will give useful information on the isotopic spin structure of the weak neutral current: this point is particularly relevant for the state $S_{11}(1505)$, which can be picked out of the cluster of resonances around 1.5 GeV by observing its large η decay mode.[6] Hence a theoretical study of I=1/2 state production seems well warranted at this time.

Throughout this paper we make the conventional assumption that the weak neutral current has a V, A spatial structure, so that weak production of the I=1/2 resonances will be closely analogous to their production in electromagnetic processes. Unfortunately, a review of the various models which have been used to theoretically calculate nucleon resonance electroproduction

shows that their predictions are not very accurate, particularly where rates are concerned.[7] At the same time, qualitative features of the electromagnetic matrix elements, such as relative signs of the amplitudes for exciting various resonances,[8] are generally correctly predicted. In view of this situation, in attempting to obtain predictions for the weak charged and neutral current excitation of $I = 1/2$ resonances, we will be guided by the following philosophy: First, we will never attempt to calculate the rate for producing one resonance relative to that for producing another, but rather will only calculate theoretically the relative rates for different forms of excitation (electromagnetic, weak charged, weak neutral) of the same resonance. Second, we will perform the calculations simultaneously in three different models which have been used for studying nucleon resonance production (the Born approximation model,[1, 9] the nonrelativistic quark model[10] and the quark bag model,[11]) and will attempt to make theoretical predictions only for those quantities for which the three models are in satisfactory agreement.

This paper is organized as follows. In Sec. 2 we define various excitation mode ratios which will be evaluated theoretically, and discuss the extraction of useful D_{13}/P_{33} and S_{11}/P_{33} excitation ratios from electroproduction data. In Sec. 3 we briefly describe the theoretical models used and tabulate the results obtained from them. The results are applied in Sec. 4 to the issues of invariant mass plot bias and resonant η production which we mentioned above. We also make an attempt to predict the D_{13}/P_{33} and S_{11}/P_{33} ratios to be expected in charged current processes, using as input the corresponding ratios observed in electroproduction. In Appendices A, B and C

we give a more detailed description of the three production models on which our theoretical estimates are based. All of the above calculations are done for the case of resonance production from free nucleon targets. In Appendix D we discuss the charge exchange corrections needed to apply the results to experiments on complex nuclear targets.

II. RATIO DEFINITIONS

In this section we introduce ratios which will enable us to compare the electromagnetic, weak charged and weak neutral current production of the P_{33}, D_{13} and S_{11} resonances. Following the standard notation for the vector and axial-vector nonet currents, we write the hadronic electromagnetic and weak charged currents (in the latter setting the Cabibbo angle θ_C to zero) as

$$\begin{aligned} \mathcal{J}^{\lambda}_{em} &= \mathcal{F}^{\lambda}_{3} + \frac{1}{\sqrt{3}}\,\mathcal{F}^{\lambda}_{8}\,, \\ \mathcal{J}^{\lambda}_{ch} &= \mathcal{F}^{\lambda}_{1+i2} - \mathcal{F}^{5\lambda}_{1+i2}\,. \end{aligned} \tag{1}$$

In calculating production matrix elements in the appendices we assume a weak neutral current with the general V, A nonet form

$$\mathcal{J}^{\lambda}_{n} = g_{V0}\mathcal{F}^{\lambda}_{0} + g_{V3}\mathcal{F}^{\lambda}_{3} + g_{V8}\mathcal{F}^{\lambda}_{8} - g_{A0}\mathcal{F}^{5\lambda}_{0} - g_{A3}\mathcal{F}^{5\lambda}_{3} - g_{A8}\mathcal{F}^{5\lambda}_{8}\,, \tag{2}$$

but in the text we immediately specialize Eq. (2) to the conventionally assumed Weinberg-Salam model current[12]

$$\mathcal{J}^{\lambda}_{n} = \mathcal{F}^{\lambda}_{3} - \mathcal{F}^{5\lambda}_{3} - 2\sin^{2}\theta_{W}\mathcal{J}^{\lambda}_{em}\,. \tag{3}$$

To proceed, let us introduce the Brookhaven National Laboratory (BNL) flux averaged cross sections for the weak charged and neutral current production

of the $D_{13}(1514)$, $S_{11}(1505)$ and $P_{33}(1232)$ resonances, and an effective cross section for their electroproduction, defined by

$$\begin{aligned}
\sigma_{ch}^{BNL}(\{\tfrac{\nu}{\bar{\nu}}\}B) &= \int dE\, n_{BNL}(E)\, \sigma_{ch}(\{\tfrac{\nu}{\bar{\nu}}\}B, E), \\
\sigma_{n}^{BNL}(\{\tfrac{\nu}{\bar{\nu}}\}B) &= \int dE\, n_{BNL}(E)\, \sigma_{n}(\{\tfrac{\nu}{\bar{\nu}}\}B, E), \\
\sigma_{em}^{BNL}(B) &= \int dE \int dt\, n_{BNL}(E)\, t^2\, \frac{d\sigma_{em}(B, E\ t)}{dt}, \\
B &= D_{13},\ S_{11} \text{ or } P_{33},\ t = -k^2 .
\end{aligned} \tag{4}$$

Here E and t denote respectively the incident lepton laboratory energy and the leptonic four-momentum transfer squared,[13] while n_{BNL} is the unit normalized Brookhaven flux, which we take as the same for incident neutrinos and antineutrinos.[14] In terms of these cross sections, we define the following ratios, which measure the amounts of D_{13} or S_{11} produced relative to the P_{33} resonance by the currents of Eqs. (1) and (3),

$$\begin{aligned}
R_{ch}^{BNL}(\nu\, B^{+}/P_{33}^{+}) &= \sigma_{ch}^{BNL}(\nu\, B^{+})/\,\sigma_{ch}^{BNL}(\nu\, P_{33}^{+}), \\
R_{ch}^{BNL}(\bar{\nu}\, B^{0}/P_{33}^{0}) &= \sigma_{ch}^{BNL}(\bar{\nu}\, B^{0})/\,\sigma_{ch}^{BNL}(\bar{\nu}\, P_{33}^{0}),
\end{aligned} \tag{5a}$$

$$\begin{aligned}
R_{n}^{BNL}(\nu\, B^{+}/P_{33}^{+}) &= \sigma_{n}^{BNL}(\nu\, B^{+})/\,\sigma_{n}^{BNL}(\nu\, P_{33}^{+}), \\
R_{n}^{BNL}(\bar{\nu}\, B^{+}/P_{33}^{+}) &= \sigma_{n}^{BNL}(\bar{\nu}\, B^{+})/\sigma_{n}^{BNL}(\bar{\nu}\, P_{33}^{+}),
\end{aligned}$$

$$\begin{aligned}
&R_{n}^{BNL}(\nu\, B^{+,0}/P_{33}^{+,0}) \\
&\quad = [\sigma_{n}^{BNL}(\nu\, B^{+}) + \sigma_{n}^{BNL}(\nu\, B^{0})]/[\sigma_{n}^{BNL}(\nu\, P_{33}^{+}) + \sigma_{n}^{BNL}(\nu\, P_{33}^{0})],
\end{aligned} \tag{5b}$$

$$\begin{aligned}
&R_{n}^{BNL}(\bar{\nu}\, B^{+,0}/P_{33}^{+,0}) \\
&\quad = [\sigma_{n}^{BNL}(\bar{\nu}\, B^{+}) + \sigma_{n}^{BNL}(\bar{\nu}\, B^{0})]/[\sigma_{n}^{BNL}(\bar{\nu}\, P_{33}^{+}) + \sigma_{n}^{BNL}(\bar{\nu}\, P_{33}^{0})],
\end{aligned}$$

$$R_{em}^{BNL}(B^+/P_{33}^+) = \sigma_{em}^{BNL}(B^+)/\sigma_{em}^{BNL}(P_{33}^+) , \qquad (5c)$$

$$B = D_{13}, S_{11} .$$

Obviously, in all cases the target charge (either proton p, neutron n or equal proton-neutron mixture p+n) can be inferred from the indicated charge superscript(s) for the produced baryon resonance.

We proceed now to rewrite Eqs. (5) so as to enable us to answer the following two basic questions: (1) Given the ratios D_{13}/P_{33} and S_{11}/P_{33} induced by the weak charged current, what are the corresponding ratios expected in weak neutral current induced processes, as a function of $\sin^2\theta_W$? (2) Given the ratios D_{13}/P_{33} and S_{11}/P_{33} observed in electroproduction on a proton target, what are the corresponding ratios expected to be induced by the weak charged current? To deal with the first question, we rearrange Eqs. (5a) and (5b) in the form

$$R_n^{BNL}(\nu B^+/P_{33}^+) = \left[\frac{R_n^{BNL}(\nu B^+/P_{33}^+)}{R_n^{BNL}(\nu B^+/P_{33}^+)\big|_{\theta_W=0}}\right]\left\{\frac{R_n^{BNL}(\nu B^+/P_{33}^+)\big|_{\theta_W=0}}{R_{ch}^{BNL}(\nu B^+/P_{33}^+)}\right\} \times R_{ch}^{BNL}(\nu B^+/P_{33}^+) ,$$

$$R_n^{BNL}(\nu B^{+,0}/P_{33}^{+,0}) = \left[\frac{R_n^{BNL}(\nu B^{+,0}/P_{33}^{+,0})}{R_n^{BNL}(\nu B^{+,0}/P_{33}^{+,0})\big|_{\theta_W=0}}\right]\left\{\frac{R_n^{BNL}(\nu B^+/P_{33}^+)\big|_{\theta_W=0}}{R_{ch}^{BNL}(\nu B^+/P_{33}^+)}\right\} \times R_{ch}^{BNL}(\nu B^+/P_{33}^+) ,$$

$$R_n^{BNL}(\bar{\nu} B^+/P_{33}^+) = \left[\frac{R_n^{BNL}(\bar{\nu} B^+/P_{33}^+)}{R_n^{BNL}(\bar{\nu} B^+/P_{33}^+)\big|_{\theta_W=0}}\right]\left\{\frac{R_n^{BNL}(\bar{\nu} B^0/P_{33}^0)\big|_{\theta_W=0}}{R_{ch}^{BNL}(\bar{\nu} B^0/P_{33}^0)}\right\} \times R_{ch}^{BNL}(\bar{\nu} B^0/P_{33}^0) \quad , \tag{6}$$

$$R_n^{BNL}(\bar{\nu} B^{+,0}/P_{33}^{+,0}) = \left[\frac{R_n^{BNL}(\bar{\nu} B^{+,0}/P_{33}^{+,0})}{R_n^{BNL}(\bar{\nu} B^{+,0}/P_{33}^{+,0})\big|_{\theta_W=0}}\right]\left\{\frac{R_n^{BNL}(\bar{\nu} B^0/P_{33}^0)\big|_{\theta_W=0}}{R_{ch}^{BNL}(\bar{\nu} B^0/P_{33}^0)}\right\} \times R_{ch}^{BNL}(\bar{\nu} B^0/P_{33}^0) \quad ,$$

$$B = D_{13}, S_{11},$$

where we have made use of the charge reflection symmetry of neutral current processes when $\theta_W = 0$. The curly brackets in Eq. (6) are all equal to a simple ratio of isospin Clebsches,

$$\left\{\frac{R_n^{BNL}(\nu B^+/P_{33}^+)\big|_{\theta_W=0}}{R_{ch}^{BNL}(\nu B^+/P_{33}^+)}\right\} = \left\{\frac{R_n^{BNL}(\bar{\nu} B^0/P_{33}^0)\big|_{\theta_W=0}}{R_{ch}^{BNL}(\bar{\nu} B^0/P_{33}^0)}\right\} = \left(\frac{\langle \frac{1}{2}\,\frac{1}{2} \,|\, 10\, \frac{1}{2}\,\frac{1}{2}\rangle}{\langle \frac{1}{2}\,\frac{1}{2} \,|\, 11\, \frac{1}{2}\,-\frac{1}{2}\rangle}\right)^2 \Big/ \left(\frac{\langle \frac{3}{2}\,\frac{1}{2} \,|\, 10\, \frac{1}{2}\,\frac{1}{2}\rangle}{\langle \frac{3}{2}\,\frac{1}{2} \,|\, 11\, \frac{1}{2}\,-\frac{1}{2}\rangle}\right)^2 = \frac{1}{4} \quad . \tag{7}$$

The square brackets in Eq. (6) involve detailed dynamical information, and will be evaluated in various production models in the next section. Since, as noted in Sec. 1, we only wish to calculate theoretical ratios relating different modes of excitation of the same resonance, we reexpress the square brackets in terms of new ratios r defined as follows,

$$r_n^{BNL}(\{\tfrac{\nu}{\bar\nu}\}B^+;\theta_W) = \sigma_n^{BNL}(\{\tfrac{\nu}{\bar\nu}\}B^+)/\sigma_n^{BNL}(\{\tfrac{\nu}{\bar\nu}\}B^+)\Big|\theta_W=0 ,$$

$$r_n^{BNL}(\{\tfrac{\nu}{\bar\nu}\}B^{+,0};\theta_W) \tag{8}$$

$$= \left[\sigma_n^{BNL}(\{\tfrac{\nu}{\bar\nu}\}B^+)+\sigma_n^{BNL}(\{\tfrac{\nu}{\bar\nu}\}B^0)\right]\Big/\left[\sigma_n^{BNL}(\{\tfrac{\nu}{\bar\nu}\}B^+)+\sigma_n^{BNL}(\{\tfrac{\nu}{\bar\nu}\}B^0)\right]\Big|\theta_W=0$$

$$B = D_{13},\ S_{11},\ P_{33} ,$$

giving the relations

$$\left[\frac{R_n^{BNL}(\nu B^+/P_{33}^+)}{R_n^{BNL}(\nu B^+/P_{33}^+)\,|\,\theta_W=0}\right] = \frac{r_n^{BNL}(\nu B^+;\theta_W)}{r_n^{BNL}(\nu P_{33}^+;\theta_W)} \quad , \text{ etc.}, \tag{9}$$

$$B = D_{13},\ S_{11}.$$

Substituting Eqs.(7) and (9) into Eq. (6) we obtain the final formulas

$$\begin{aligned}
R_n^{BNL}(\nu B^+/P_{33}^+) &= \tfrac{1}{4}\,\frac{r_n^{BNL}(\nu B^+;\theta_W)}{r_n^{BNL}(\nu P_{33}^+;\theta_W)}\,R_{ch}^{BNL}(\nu B^+/P_{33}^+) ,\\
R_n^{BNL}(\nu B^{+,0}/P_{33}^{+,0}) &= \tfrac{1}{4}\,\frac{r_n^{BNL}(\nu B^{+,0};\theta_W)}{r_n^{BNL}(\nu P_{33}^{+,0};\theta_W)}\,R_{ch}^{BNL}(\nu B^+/P_{33}^+) ,\\
R_n^{BNL}(\bar\nu B^+/P_{33}^+) &= \tfrac{1}{4}\,\frac{r_n^{BNL}(\bar\nu B^+;\theta_W)}{r_n^{BNL}(\bar\nu P_{33}^+;\theta_W)}\,R_{ch}^{BNL}(\bar\nu B^0/P_{33}^0) ,\\
R_n^{BNL}(\bar\nu B^{+,0}/P_{33}^{+,0}) &= \tfrac{1}{4}\,\frac{r_n^{BNL}(\bar\nu B^{+,0};\theta_W)}{r_n^{BNL}(\bar\nu P_{33}^{+,0};\theta_W)}\,R_{ch}^{BNL}(\bar\nu B^0/P_{33}^0) ,
\end{aligned} \tag{10}$$

$$B = D_{13},\ S_{11}.$$

To deal with the second question we follow a closely analogous procedure, of which we state only the result. Letting $\sigma^{BNL}(\nu B;\mathcal{J})$

denote the flux averaged cross section for production of the resonance B by the weak current $\mathcal{J}$, we define the ratios

$$r^{BNL}_{va/em}(\nu B^+) = \sigma^{BNL}(\nu B^+; \mathcal{J}^{\lambda}_3 - \mathcal{J}^{5\lambda}_3) / \sigma^{BNL}(\nu B^+; \mathcal{J}^{\lambda}_3 + \frac{1}{\sqrt{3}} \mathcal{J}^{\lambda}_8) ,$$

$$r^{BNL}_{ch\,\bar{\nu}/\nu}(B) = \sigma^{BNL}_{ch}(\bar{\nu} B^0) / \sigma^{BNL}_{ch}(\nu B^+) , \tag{11}$$

$$B = D_{13}, S_{11}, P_{33} .$$

In terms of these quantities, which again compare only different production modes for the same resonance, the relation between Eqs. (5a) and Eq. (5c) takes the form

$$R^{BNL}_{ch}(\nu B^+/P^+_{33}) = 4 \frac{r^{BNL}_{va/em}(\nu B^+)}{r^{BNL}_{va/em}(\nu P^+_{33})} R^{BNL}_{em}(B^+/P^+_{33}) ,$$

$$R^{BNL}_{ch}(\bar{\nu} B^0/P^0_{33}) = \frac{r^{BNL}_{ch\,\bar{\nu}/\nu}(B)}{r^{BNL}_{ch\,\bar{\nu}/\nu}(P_{33})} R^{BNL}_{ch}(\nu B^+/P^+_{33}) , \tag{12}$$

$$B = D_{13}, S_{11} .$$

We conclude this section by outlining the calculation of the ratios $R^{BNL}_{em}(D^+_{13}/P^+_{33})$ and $R^{BNL}_{em}(S^+_{11}/P^+_{33})$ from electroproduction data, employing a detailed survey of the electroproduction of nucleon resonances which has been given recently by Devenish and Lyth.[15] In Table IA we summarize the values given by these authors for the masses and widths of the lowest lying resonances. Although the Roper P_{11} resonance is included in this table, Devenish and Lyth find that the electroproduction

of this state is effectively zero, and so we ignore it throughout this paper.[16] For the resonances D_{13}, S_{11} and P_{33} we assume that the transverse electroproduction cross section σ_T is dominant and ignore the longitudinal cross section σ_L, an approximation which should be good to an accuracy of roughly 30%.[15] Making this assumption, we get from the graphs of Ref. 15 and from an earlier summary of Clegg[17] the transverse electroproduction cross sections at resonance peak, denoted by $\sigma_T(B, t)$, which are tabulated in Table IB. From these the electroproduction cross sections $d\sigma_{em}(B, E\,t)/dt$ which appear in Eq. (4) are obtained by

$$t^2 \frac{d\sigma_{em}(B, E\,t)}{dt} = \text{CONST} \times \frac{\Gamma_B M_B (M_B^2 - M_N^2)}{E^2} \left[1 + \frac{2k_{10}k_{20}\cos^2(\theta/2)}{|\vec{k}|^2} \right] \sigma_T(B, t) , \tag{13}$$

with M_N the nucleon mass and with k_{10}, k_{20}, $|\vec{k}|$ and θ the initial lepton energy, final lepton energy, lepton three momentum transfer and lepton scattering angle in the B rest frame,

$$\begin{aligned} k_{20} &= \frac{M_N^2 + 2M_N E - M_B^2}{2M_B} , \\ k_{10} &= k_{20} + k_0 , \quad k_0 = \frac{M_B^2 - M_N^2 - t}{2M_B} , \\ |\vec{k}| &= [t + k_0^2]^{\frac{1}{2}} , \\ \sin^2 \frac{\theta}{2} &= t/(4\,k_{10}k_{20}). \end{aligned} \tag{14}$$

Performing the numerical integration of Eq. (4) using the data tabulated in Table I, we find

$$R_{em}(D_{13}^{+}/P_{33}^{+}) \approx 0.50 \ ,$$
$$R_{em}(S_{11}^{+}/P_{33}^{+}) \approx 0.13 \ . \qquad (15)$$

III. MODEL CALCULATIONS

To obtain theoretical predictions for the ratios r defined in the preceding section, we have performed calculations using three different models for resonance production. The first model, which we call the Born approximation model,[1, 9] approximates the multipoles describing the process $\gamma + N \to B \to \pi + N$ by their Born approximations,[18] multiplied by a suitable W-dependent but k^2-independent unitarization factor. (The model ignores all channels other than the πN channel, even though some of them are obviously important). In the narrow resonance approximation this unitarization factor divides out in our applications, and so only the Born approximations, arising from the Feynman diagrams of Fig. 1, are needed. We have evaluated this model in two different forms, which respectively omit or include the ω-exchange diagram of Fig. 1. The results obtained from the two forms, as we shall see, are quite similar. Further details of this model, and the evaluation of the coupling parameters appearing in the ω-exchange diagram, are described in Appendix A.

The second model used is the standard nonrelativistic quark model,[10] which we evaluated both with mixing of the $8^{3/2}$ into the $8^{1/2}$ configuration (using the parameters summarized by Hey, Litchfield and Cashmore[19]) and

also without mixing, with results nearly independent of which form is used. Further details of the calculations in this model are described in Appendix B. The third model used is the quark bag model,[11] which is calculationally similar to the usual quark model but differs from it in its wave function assignments for the D_{13} and S_{11} states. In this model no mixing occurs for the D_{13} state, but there are two possible wave function assignments, which we have labeled #1 and #2, for the S_{11} state. Since no determination of the mixing angle has been made yet in this model, we have surveyed the set of angles -60°, -45°, -30°, 0°, 30°, 45°, 60°, 90°. Details of the quark bag calculation, and of the dependence of the results on mixing angle, are given in Appendix C.

Numerical results of our calculations in the three models are summarized in Tables II, III and IV, which give respectively the ratios r_n^{BNL}, $r_{va/em}^{BNL}$ and $r_{ch\ \bar{\nu}/\nu}^{BNL}$. From Table II we see that the three models give reasonably consistent results in the case of r_n^{BNL}, particularly for incident neutrinos, with similar results obtained for all three resonant states. From Table IV we see that the isovector vector-axial vector interference in a neutrino beam is constructive for the D_{13} and S_{11} states, just as it is for weak production of the P_{33} resonance; in this case again the three models give nicely consistent results. Turning to the ratios $r_{va/em}^{BNL}$ tabulated in Table III, we see that although the three models continue to agree well in their predictions for the P_{33} state, the agreement for the D_{13} and S_{11} states is poor. In particular, an infinite prediction for $r_{va/em}^{BNL}(D_{13}^+)$ in the bag model arises because (as has already been noted by Donoghue et al.[11]) the

reaction $\gamma + p \to D_{13}^{+}$ is forbidden in this model.[20] Even leaving the quark bag model aside, the agreement between the standard quark model and the Born approximation model is not good in the case of the ratios $r_{va/em}^{BNL}$.

IV. APPLICATIONS AND DISCUSSION

Armed with the numerical results of the preceding section, we return now to the issues raised in Sec. 1. Substituting the values of r_n from Table II into Eq. (10), we find for the ratios $R_n^{BNL}(\nu B^{+}/P_{33}^{+})/R_{ch}^{BNL}(\nu B^{+}/P_{33}^{+})$ the results summarized in Table V. These ratios measure the prominence of the $I = 1/2$ resonances (relative to the P_{33}) in neutral current reactions, as compared with their prominence (again relative to the P_{33}) in the charged current case. We see that[16] in the Weinberg-Salam model, with $\sin^2\theta_W$ in the range of experimental interest, the three production models all predict that the ratios D_{13}/P_{33} and S_{11}/P_{33} observed on free nucleon targets are at least a factor of two smaller in the neutral current than in the charged current case. As a result, if the $I=1/2$ resonances are found not to distort seriously invariant mass plots in the charged current case, they should not be expected to do so in the neutral current case. Furthermore, the production of η's from the S_{11} relative to the P_{33} should be smaller by a factor of two or more in the neutral current than in the charged current case. The modifications to these conclusions resulting from charge exchange corrections in complex nuclear targets are given in Appendix D.

Substituting the values of $r_{va/em}$ from Table III into Eq. (12), we get for the ratios $R_{ch}^{BNL}(\nu\, B^+/P_{33}^+)/R_{em}^{BNL}(B^+/P_{33}^+)$ the results summarized in Table VI. The predictions of the three models in this case are not in good accord, and so we cannot extract from the electroproduction data of Eq. (15) a firm result for the ratios D_{13}/P_{33} and S_{11}/P_{33} to be expected in charged current reactions. The best that can be said is that based on the models, the resonance production ratios might be expected to lie in the ranges

$$\begin{aligned} 0.8 \;\lesssim\; R_{ch}^{BNL}(\nu\, D_{13}^+/P_{33}^+) \;\lesssim\; 2.6 \\ 0.2 \;\lesssim\; R_{ch}^{BNL}(\nu\, S_{11}^+/P_{33}^+) \;\lesssim\; 1.0\,, \end{aligned} \tag{16}$$

with the lower ends of the ranges favoring the quark model values and the upper ends favoring the Born approximation model values.

ACKNOWLEDGMENTS

We wish to thank Professors B. W. Lee and W. Lee for asking the questions which stimulated this investigation.

APPENDIX A

We give in this Appendix further details of the Born approximation model for resonance production, which has been briefly described in Sec. 3. We follow closely the notation[21] of Ref. 1, which gives an extended discussion of the kinematics of weak pion production, with a particular emphasis on $P_{33}(1232)$ production. As we have already noted, in the Born approximation model the multipoles for resonance production are equated to the Born approximations projected from the diagrams of Fig. 1, times a unitarization factor (calculated ignoring all channels other than the πN channel) which divides out in our applications. The relevant multipoles may be read off from the cross section formulas for neutrino induced resonance excitation,

$$\frac{d\sigma(D_{13}, E\,k^2)}{d(k^2)} = \text{CONST} \times \frac{|\vec{q}|}{E^2} \{f_1[4(|E_{2-}|^2 + |\mathcal{M}_{2-}|^2) + 12(|M_{2-}|^2 + |\mathcal{C}_{2-}|^2)]$$
$$+ f_2\, 8[k_0^2 |\mathcal{L}_{2-}|^2 + (k^2/k_0)^2 |L_{2-}|^2]$$
$$+ f_3\, \mathrm{Re}[-4E_{2-}\mathcal{M}^*_{2-} + 12M_{2-}\mathcal{C}^*_{2-}]\}\ ,$$

$$\frac{d\sigma(S_{11}, E\,k^2)}{d(k^2)} = \text{CONST} \times \frac{|\vec{q}|}{E^2} \{f_1\, 2(|E_{0+}|^2 + |\mathcal{M}_{0+}|^2)$$
$$+ f_2[k_0^2 |\mathcal{L}_{0+}|^2 + (k^2/k_0)^2 |L_{0+}|^2]$$
$$+ f_3\, \mathrm{Re}(2E_{0+}\mathcal{M}^*_{0+})\}\ ,$$

$$\frac{d\sigma(P_{33}, E\,k^2)}{d(k^2)} = \text{CONST} \times \frac{|\bar{q}|}{E^2} \{ f_1[4(|M_{1+}|^2 + |\mathcal{E}_{1+}|^2) + 12(|E_{1+}|^2 + |\mathcal{M}_{1+}|^2)]$$

$$+ f_2\, 8[k_0^2\, |\mathcal{L}_{1+}|^2 + (k^2/k_0)^2\, |L_{1+}|^2] \qquad \text{(A.1)}$$

$$+ f_3\, \mathrm{Re}[-4M_{1+}\mathcal{E}^*_{1+} + 12E_{1+}\mathcal{M}^*_{1+}] \} ,$$

$$f_1 = \tfrac{1}{2} k^2 [1 + 2 k_{10} k_{20} \cos^2(\theta/2)/|\bar{k}|^2] ,$$

$$f_2 = 2 k_{10} k_{20} \cos^2(\theta/2)/|\bar{k}|^2 , \qquad f_3 = \xi (k_{10} + k_{20}) k^2/|\bar{k}| ,$$

$$\xi = \begin{cases} +1 & \nu \text{ incident} \\ -1 & \bar{\nu} \text{ incident} \end{cases} ,$$

$$|\bar{q}| = (q_0^2 - M_\pi^2)^{\frac{1}{2}} , \quad q_0 = (M_B^2 - M_N^2 + M_\pi^2)/(2M_B) .$$

For neutral-current induced reactions, the vector multipoles $V \equiv M, E, L$ and the axial-vector multipoles $\mathcal{A} \equiv \mathcal{M}, \mathcal{E}, \mathcal{L}$ appearing in Eq. (A.1) are related to the multipoles with definite isospin character $V^{(\frac{1}{2}, 0)}$, $\mathcal{A}^{(\frac{1}{2}, 0)}$ and the isospin coefficients $a_E^{(\frac{1}{2})}$, defined as in Ref. 1, by

$$V = a_E^{(\frac{1}{2})} [\varepsilon\, g_{V3}\, V^{(\frac{1}{2})} + 9\, g_{VS}\, V^{(0)}] ,$$

$$\mathcal{A} = a_E^{(\frac{1}{2})} [\varepsilon\, g_{A3} \mathcal{A}^{(\frac{1}{2})} + 3\, g_{AS} \mathcal{A}^{(0)}] , \qquad \text{(A.2)}$$

$$g_{VS} \equiv \left(\frac{2}{3}\right)^{\frac{1}{2}} g_{V0} + \left(\frac{1}{3}\right)^{\frac{1}{2}} g_{V8} ,$$

$$g_{AS} \equiv \left(\frac{2}{3}\right)^{\frac{1}{2}} g_{A0} + \left(\frac{1}{3}\right)^{\frac{1}{2}} g_{A8} , \quad \varepsilon = \begin{cases} +1 & \text{p target} \\ -1 & \text{n target} \end{cases} .$$

In terms of invariant amplitudes, the Born approximation associated with Fig. 1 is completely specified by Eqs. (2E.5) and (2E.6) of Ref. 1 and the

following expressions for the nonvanishing axial isoscalar and the ω-exchange amplitudes,[21]

$$A_1^{(0)B} = g_r \frac{g_A^S(k^2)}{2M_N}\left(\frac{1}{\nu_B - \nu} - \frac{1}{\nu_B + \nu}\right),$$

$$A_3^{(0)B} = g_r \frac{g_A^S(k^2)}{2M_N}\left(\frac{1}{\nu_B - \nu} + \frac{1}{\nu_B + \nu}\right), \qquad \text{(A. 3)}$$

$$\Delta V_{4\omega}^{(+)B} = \frac{2\, g_{\omega\pi\gamma}\, g_{\omega NN}\, D(k^2)}{k^2 - 4M_N\nu_B + m_\omega^2 - M_\pi^2}.$$

Here $g_r \approx 13.4$ is the pion-nucleon coupling constant, $g_{\omega\pi\gamma}$ and $g_{\omega NN}$ are (as indicated) ω-exchange coupling constants, and $D(k^2)$ is a form factor which we take as[22] $[1+k^2/(0.9\,\mathrm{GeV})^2]^{-1}$ in the numerical work. In addition to including the Born amplitudes per se, we have also included in the model the following additions which bring the Born amplitude into agreement with fourth order soft pion theorems,[23]

$$\Delta V_1^{(+)} = \frac{g_r}{M_N} F_2^V(k^2),$$

$$\Delta V_1^{(0)} = \frac{g_r}{M_N} F_2^S(k^2),$$

$$\Delta V_6^{(-)} = \frac{g_r}{M_N}\frac{1}{k^2}\left[\frac{g_A(k^2)}{g_A(0)} - F_1^V(k^2)\right], \qquad \text{(A. 4)}$$

$$\Delta A_2^{(-)} = \frac{g_r}{M_N g_A(0)} F_2^V(k^2),$$

$$\Delta A_4^{(-)} = -\frac{g_r}{M_N^2 g_A(0)}\left[F_1^V(k^2) - g_A(0)\, g_A(k^2) + 2M_N F_2^V(k^2)\right].$$

Starting from the invariant amplitudes, the Born approximations to the multipoles appearing in Eq. (A. 1) were calculated algebraically using the equations

in Appendices 1-3 of Ref. 1, and were checked against an independent calculation by numerical integration.

In the numerical calculations within the framework of the Weinberg-Salam model described in the text, the isoscalar axial-vector form factor $g_A^S(k^2)$ does not appear.[24] For the ω-exchange parameters, we used the following estimates. First, assuming ω-dominance of the nucleon form factor $F_1^S(k^2)$ (the ϕ-nucleon coupling is very weak) gives the relations[9]

$$\frac{g_{\omega\gamma}\, g_{\omega NN}}{m_\omega^2} \cdot \frac{1}{1 + \frac{k^2}{m_\omega^2}} \approx \tfrac{1}{2} F_1^S(k^2) \ , \qquad \frac{g_{\omega\gamma}\, g_{\omega NN}}{m_\omega^2} \approx \tfrac{1}{2} \ , \tag{A.5}$$

while the formulas[25] (α is the fine structure constant)

$$\Gamma(\omega \to \pi\gamma) = \frac{\alpha\, m_\omega^3}{24} g_{\omega\pi\gamma}^2 \left(1 - \frac{M_\pi^2}{m_\omega^2}\right)^3 = 0.89 \pm 0.05 \text{ MeV} \ ,$$

$$\Gamma(\omega \to e^+e^-) = \frac{4}{3}\pi\alpha^2 m_\omega \left(\frac{g_{\omega\gamma}}{m_\omega^2}\right)^2 = 0.76 \pm 0.03 \text{ keV} \ , \tag{A.6}$$

imply the coupling constant values

$$g_{\omega\pi\gamma} = (2.58 \pm 0.13)\ (\text{GeV})^{-1} \ ,$$

$$\frac{g_{\omega\gamma}}{m_\omega^2} = 0.066 \pm 0.004 \ . \tag{A.7}$$

Combining Eqs. (A. 5) and (A. 7) gives then the estimate

$$|g_{\omega\pi\gamma}\, g_{\omega NN}| = (3.11 \pm 0.22)\, M_\pi^{-1} \,. \qquad \text{(A. 8)}$$

To determine the sign of $g_{\omega\pi\gamma}\, g_{\omega NN}$, we note that in the limit $m_\omega \to 0$ the vector meson-photon analogy becomes exact, and the ω-exchange diagram of Fig. 1 becomes identical to the Primakoff diagram for π^0 photoproduction. Comparison with the known sign[26] of the amplitude $F(\pi^0 \to 2\gamma)$ relative to g_r then indicates that for positive g_r, the product $g_{\omega\pi\gamma}\, g_{\omega NN}$ is also positive, and so we have finally

$$g_{\omega\pi\gamma}\, g_{\omega NN} = +(3.11 \pm 0.22)\, M_\pi^{-1} \,. \qquad \text{(A. 9)}$$

In terms of the parameter β used by Walecka and Zucker[9] to describe the ω-exchange contribution to pion electroproduction, Eq. (A. 9) corresponds to[27]

$$\beta = 1.68 \pm 0.12 \,. \qquad \text{(A. 10)}$$

APPENDIX B

We give here details of the nonrelativistic harmonic oscillator quark model for resonance production. Our calculations follow closely the work of Faiman and Hendry[10] and Abdullah and Close.[10] We work throughout in the Breit frame,[10] where the initial and final lepton energies k_{10}^*, k_{20}^*, the lepton three momentum transfer $|\vec{k}^*|$ and the lepton scattering angle θ^* are given by

$$k_{10}^* = \frac{2M_N E - \frac{1}{2}t}{[2(M_N^2 + M_B^2) + t]^{\frac{1}{2}}}, \qquad k_{20}^* = \frac{2M_N E + M_N^2 - M_B^2 - \frac{1}{2}t}{[2(M_N^2 + M_B^2) + t]^{\frac{1}{2}}},$$

$$k^* \equiv |\vec{k}^*| = \left[t + \frac{(M_B^2 - M_N^2)^2}{2(M_B^2 + M_N^2) + t} \right]^{\frac{1}{2}}, \quad \sin^2(\tfrac{1}{2}\theta^*) = t/(4k_{10}^* k_{20}^*). \tag{B.1}$$

In constructing the $I = \frac{1}{2}$ resonance wave functions, we allow at the outset for mixing of the quark spin 3/2 states in the baryon 70 representation of SU_6 into the states with quark spin 1/2, according to the recipe

$$S_{11}(1505) = \cos\theta_S \, S_{11}(8^{1/2}) - \sin\theta_S \, S_{11}(8^{3/2}),$$

$$D_{13}(1514) = \cos\theta_D \, D_{13}(8^{1/2}) - \sin\theta_D \, D_{13}(8^{3/2}). \tag{B.2}$$

For the (overall totally symmetric) wave functions of states with angular momentum component S we take

$$\psi[p(938);\tfrac{1}{2}S] = \frac{1}{2^{\frac{1}{2}}}\psi_0^O[\,|\tfrac{1}{2}S>_\alpha \psi_\alpha(\mathcal{SSN}) + |\tfrac{1}{2}S>_\beta \psi_\beta(\mathcal{SSN})\,],$$

$$\psi[P_{33}^+(1232);\tfrac{3}{2}S] = \psi_0^O\,|\tfrac{3}{2}S>_S\,\psi_S(\mathcal{SSN}),$$

$$\psi[B^+(8^{1/2});JS] = \sum_{M,s} <JS|1M\tfrac{1}{2}s>\,\psi(1M\tfrac{1}{2}s),$$

$$\psi[B^+(8^{3/2});JS] = \sum_{M,s} <JS|\tfrac{3}{2}s1M>\,\psi(1M\tfrac{3}{2}s),$$

$$J = \begin{cases} \frac{3}{2} & \text{for } B = D_{13} \\ \frac{1}{2} & \text{for } B = S_{11} \end{cases}, \qquad \text{(B.3)}$$

$$\psi(1M\tfrac{1}{2}s) = \tfrac{1}{2}\psi_\alpha^O(1M)\,[-|\tfrac{1}{2}s>_\alpha \psi_\alpha(\mathcal{SSN}) + |\tfrac{1}{2}s>_\beta \psi_\beta(\mathcal{SSN})]$$

$$+ \tfrac{1}{2}\psi_\beta^O(1M)\,[\,|\tfrac{1}{2}s>_\alpha \psi_\beta(\mathcal{SSN}) + |\tfrac{1}{2}s>_\beta \psi_\alpha(\mathcal{SSN})\,],$$

$$\psi(1M\tfrac{3}{2}s) = \frac{1}{2^{\frac{1}{2}}}\,[\psi_\alpha^O(1M)\,|\tfrac{3}{2}s>_S\,\psi_\alpha(\mathcal{SSN}) + \psi_\beta^O(1M)\,|\tfrac{3}{2}s>_S\,\psi_\beta(\mathcal{SSN})\,],$$

with the α and β states bases for the mixed symmetry representation of S_3. The orbital wave functions ψ^O appearing in Eq. (B.3) are given by

$$\psi_0^O = N_0 \exp[-\tfrac{1}{2}\delta^2(\bar{\lambda}^2+\bar{\rho}^2)]\,\exp(i\bar{P}\cdot\bar{R}),$$

$$\psi_\alpha^O\begin{pmatrix}1 & 0\\ \pm 1\end{pmatrix} = N_1 \exp[-\tfrac{1}{2}\delta^2(\bar{\lambda}^2+\bar{\rho}^2)]\,\exp(i\bar{P}\cdot\bar{R})\begin{pmatrix}\lambda_z\\ \mp\frac{1}{2^{\frac{1}{2}}}(\lambda_x \pm i\lambda_y)\end{pmatrix},$$

$$\psi_\beta^O\begin{pmatrix}1 & 0\\ \pm 1\end{pmatrix} = N_1 \exp[-\tfrac{1}{2}\delta^2(\bar{\lambda}^2+\bar{\rho}^2)]\,\exp(i\bar{P}\cdot\bar{R})\begin{pmatrix}\rho_z\\ \mp\frac{1}{2^{\frac{1}{2}}}(\rho_x \pm i\rho_y)\end{pmatrix},$$

$$N_0 = \delta^3/(\pi^3\,2^{3/2}\,3^{3/4}),\quad N_1 = 2^{1/2}\,\delta\,N_0, \qquad \text{(B.4a)}$$

with the center-of-mass coordinate $\bar{R}$ and the relative coordinates $\bar{\lambda}$, $\bar{\rho}$

given in terms of quark coordinates $\vec{r}_{1,2,3}$ by

$$\vec{R} = \frac{1}{3}(\vec{r}_1 + \vec{r}_2 + \vec{r}_3),$$

$$\vec{\lambda} = \frac{1}{\sqrt{6}\delta}(\vec{r}_1 + \vec{r}_2 - 2\vec{r}_3), \qquad \vec{r} = \frac{1}{2\delta}(\vec{r}_1 - \vec{r}_2), \tag{B.4}$$

and with δ a parameter related to the oscillator frequency. The orbital wave functions have been normalized so that

$$\int d^3r_1\, d^3r_2\, d^3r_3\ \psi_f^{O*}\ \psi_i^O = \delta^3(\vec{P}_f - \vec{P}_i), \tag{B.5}$$

with $\vec{P}$ the total momentum. The spin wave functions $|\frac{1}{2}s\rangle_{\alpha,\beta}$ and $|\frac{3}{2}s\rangle_S$, and the SU_3 wave functions $\psi_{\alpha,\beta}(\Omega\Omega\Omega_\lambda)$ and $\psi_S(\Omega\Omega\Omega)$ are given by

$$|\tfrac{1}{2}\tfrac{1}{2}\rangle_\alpha = \psi_\alpha(\uparrow\uparrow\downarrow) \qquad |\tfrac{1}{2}-\tfrac{1}{2}\rangle_\alpha = -\psi_\alpha(\downarrow\downarrow\uparrow)$$

$$|\tfrac{1}{2}\tfrac{1}{2}\rangle_\beta = \psi_\beta(\uparrow\uparrow\downarrow) \qquad |\tfrac{1}{2}-\tfrac{1}{2}\rangle_\beta = -\psi_\beta(\downarrow\downarrow\uparrow),$$

$$|\tfrac{3}{2}\tfrac{3}{2}\rangle_S = \psi_S(\uparrow\uparrow\uparrow), \tag{B.6}$$

$$|\tfrac{3}{2}\tfrac{1}{2}\rangle_S = \psi_S(\uparrow\uparrow\downarrow),$$

$$|\tfrac{3}{2}-\tfrac{1}{2}\rangle_S = \psi_S(\uparrow\downarrow\downarrow),$$

$$|\tfrac{3}{2}-\tfrac{3}{2}\rangle_S = \psi_S(\downarrow\downarrow\downarrow),$$

with

$$\psi_S(xyz) = \frac{1}{6^{\frac{1}{2}}}\left[\,|xyz\rangle + |xzy\rangle + |yxz\rangle + |yzx\rangle + |zxy\rangle + |zyx\rangle\right],$$

$$\psi_\alpha(xxz) = \frac{1}{6^{\frac{1}{2}}}\left[\,|zxx\rangle + |xzx\rangle - 2|xxz\rangle\right], \qquad \text{(B. 6b)}$$

$$\psi_\beta(xxz) = \frac{1}{2^{\frac{1}{2}}}\left[\,|zxx\rangle - |xzx\rangle\right]$$

denoting the symmetric and mixed states of the quark spin or internal symmetry variables. Note that according to our conventions, the state $|xyz\rangle$ is a product state in which quark 1 is in state x, quark 2 is in state y and quark 3 is in state z.

Letting W_λ denote the lepton current

$$W_\lambda = \frac{G}{2^{\frac{1}{2}}}\,\bar{\nu}(k_2)\,\gamma_\lambda(1-\gamma_5)\,\nu(k_1)\,, \qquad \text{(B. 7)}$$

we proceed now to evaluate quark model matrix elements of the interaction operator

$$\mathcal{M} = W_\lambda \mathcal{J}^\lambda_n = \sum_{\text{quark } i} \mathcal{M}_{(i)}\,. \qquad \text{(B. 8)}$$

Since the wave functions are symmetric with respect to the three quarks, it suffices to keep only one of the three terms in Eq. (B. 8) and then to multiply the amplitude at the end by a factor of 3. It proves convenient to keep the $i = 3$ piece, since then the overlap integrals involving the β-type orbital wavefunctions are zero as a result of their antisymmetry in the 1 and 2 variables. Taking the nonrelativistic limit of $\mathcal{M}_{(3)}$, we find (with $\bar{r}$, $\bar{p}$, $\bar{\sigma}$ and λ_j understood to be, respectively, the coordinate, canonical momentum, Pauli spin matrix and SU_3 matrix for the third quark, taking the z axis to lie along the lepton momentum transfer $\bar{k}^*$, and letting M_q denote the quark mass),

$$\mathcal{M} \sim 3\mathcal{M}_{(3)}$$

$$\underset{\text{non-relativistic limit}}{=} 3e^{ik^* r_z} \sum_{j=0,3,8} \left\{ W_0 g_{Vj} \tfrac{1}{2}\lambda_j - \frac{2^{\frac{1}{2}} W_0}{M_q} g_{Aj} \tfrac{1}{2}\lambda_j \left[\frac{1}{2^{\frac{1}{2}}} \sigma_z \tilde{p}_z + \sigma_+ p_- + \sigma_- p_+ \right] - \frac{g_{Vj} \tfrac{1}{2}\lambda_j}{M_q} \left[W_z \tilde{p}_z + W_+ p_- + W_- p_+ \right] \right.$$

$$\left. - \frac{g_{Vj} \tfrac{1}{2}\lambda_j k^*}{2^{\frac{1}{2}} M_q} (\sigma_+ W_- - \sigma_- W_+) + 2^{\frac{1}{2}} g_{Aj} \tfrac{1}{2}\lambda_j \left[\frac{\sigma_z W_z}{2^{\frac{1}{2}}} + \sigma_+ W_- + \sigma_- W_+ \right] \right\} , \tag{B.9}$$

$$\tilde{p}_z = p_z + \tfrac{1}{2} k^* \hat{z}, \quad p_\pm = 2^{-\frac{1}{2}}(p_x \pm i p_y), \quad \sigma_\pm = \tfrac{1}{2}(\sigma_x \pm i \sigma_y) ,$$

$$W_0 = \frac{G}{m_\nu} (2 k_{10}^* k_{20}^*)^{\frac{1}{2}} \cos(\tfrac{1}{2}\theta^*) ,$$

$$W_z = \frac{G}{m_\nu} (2 k_{10}^* k_{20}^*)^{\frac{1}{2}} \frac{(k_{10}^* - k_{20}^*)}{k^*} \cos(\tfrac{1}{2}\theta^*) ,$$

$$W_\pm = \frac{1}{2^{\frac{1}{2}}} (W_x \pm i W_y) = \frac{G}{m_\nu} (k_{10}^* k_{20}^*)^{\frac{1}{2}} \frac{k_{10}^* + k_{20}^* \pm k^*}{k^*} \sin(\tfrac{1}{2}\theta^*) .$$

On taking matrix elements of Eq. (B.9) using the wave functions constructed above, we find (quantizing spins along the z axis)

$$\langle D_{13}, S = \tfrac{3}{2} | \mathcal{M} | p, S = \tfrac{1}{2} \rangle$$

$$= \frac{\cos\theta_D}{2^{\frac{1}{2}}} \frac{I_3}{M_q} W_- g_{V3} + \frac{3}{2} \frac{\sin\theta_D}{5^{\frac{1}{2}}} I_2 W_- \left[(\tfrac{1}{2}k^*/M_q)(g_{VS} - \tfrac{1}{3} g_{V3}) - (g_{AS} - \tfrac{1}{3} g_{A3}) \right] ,$$

$$\langle D_{13}, S = \tfrac{1}{2} | \mathcal{M} | p, S = \tfrac{1}{2} \rangle$$

$$= \frac{\cos\theta_D}{3^{\frac{1}{2}}} I_2 \left[W_0 g_{V3} + W_z (g_{AS} + \frac{2}{3} g_{A3}) \right] - \frac{\cos\theta_D}{3^{\frac{1}{2}}} \frac{I_3}{M_q} W_z g_{V3} + \frac{\sin\theta_D}{(30)^{\frac{1}{2}}} I_2 W_z (g_{AS} - \tfrac{1}{3} g_{A3}$$

$$\langle D_{13},\ S=-\tfrac{1}{2}\ |\mathcal{M}|\ p,\ S=\tfrac{1}{2}\rangle$$

$$= -\frac{\cos\theta_D}{6^{\frac{1}{2}}}\frac{I_3}{M_q}\,W_+\,g_{V3} + 2\,\frac{\cos\theta_D}{6^{\frac{1}{2}}}\,I_2\,W_+\left[(\tfrac{1}{2}k^*/M_q)(g_{VS}+\tfrac{2}{3}g_{V3})+g_{AS}+\tfrac{2}{3}g_{A3}\right]$$

$$-\tfrac{1}{2}\,\frac{\sin\theta_D}{(15)^{\frac{1}{2}}}\,I_2\,W_+\left[(\tfrac{1}{2}k^*/M_q)(g_{VS}-\tfrac{1}{3}g_{V3})+g_{AS}-\tfrac{1}{3}g_{A3}\right],$$

$$\langle D_{13},\ S=-\tfrac{3}{2}\ |\mathcal{M}|\ p,\ S=\tfrac{1}{2}\rangle = 0\ ; \qquad \text{(B.10a)}$$

$$\langle S_{11},\ S=\tfrac{1}{2}\ |\mathcal{M}|\ p,\ S=\tfrac{1}{2}\rangle$$

$$= \frac{\cos\theta_S}{6^{\frac{1}{2}}}\frac{I_3}{M_q}\left[W_z\,g_{V3}+3\,W_0(g_{AS}+\tfrac{2}{3}g_{A3})\right]$$

$$-\frac{\cos\theta_S}{6^{\frac{1}{2}}}\,I_2\left[W_0\,g_{V3}+W_z(g_{AS}+\tfrac{2}{3}g_{A3})\right]+\frac{\sin\theta_S}{6^{\frac{1}{2}}}\,I_2\,W_z(g_{AS}-\tfrac{1}{3}g_{A3})$$

$$-3\,\frac{\sin\theta_S}{6^{\frac{1}{2}}}\frac{I_3}{M_q}\,W_0(g_{AS}-\tfrac{1}{3}g_{A3}),$$

$$\langle S_{11},\ S=-\tfrac{1}{2}\ |\mathcal{M}|\ p,\ S=\tfrac{1}{2}\rangle$$

$$= \frac{\cos\theta_S}{3^{\frac{1}{2}}}\frac{I_3}{M_q}\,W_+\,g_{V3}+\frac{\cos\theta_S}{3^{\frac{1}{2}}}\,I_2\,W_+\left[(\tfrac{1}{2}k^*/M_q)(g_{VS}+\tfrac{2}{3}g_{V3})+g_{AS}+\tfrac{2}{3}g_{A3}\right]$$

$$+\tfrac{1}{2}\,\frac{\sin\theta_S}{3^{\frac{1}{2}}}\,I_2\,W_+\left[(\tfrac{1}{2}k^*/M_q)(g_{VS}-\tfrac{1}{3}g_{V3})+g_{AS}-\tfrac{1}{3}g_{A3}\right]; \qquad \text{(B.10b)}$$

$$\langle P_{33},\ S=\tfrac{3}{2}\ |\mathcal{M}|\ p,\ S=\tfrac{1}{2}\rangle = -\frac{2}{3^{\frac{1}{2}}}\,I_0\,W_-\left[-(\tfrac{1}{2}k^*/M_q)\,g_{V3}+g_{A3}\right],$$

$$\langle P_{33},\ S=\tfrac{1}{2}\ |\mathcal{M}|\ p,\ S=\tfrac{1}{2}\rangle = \frac{2^{3/2}}{3}\,I_0\,W_z\,g_{A3},$$

$$\langle P_{33},\ S=-\tfrac{1}{2}\ |\mathcal{M}|\ p,\ S=\tfrac{1}{2}\rangle = \frac{2}{3}\,I_0\,W_+\left[(\tfrac{1}{2}k^*/M_q)\,g_{V3}+g_{A3}\right],$$

$$\langle P_{33},\ S=-\tfrac{3}{2}\ |\mathcal{M}|\ p,\ S=\tfrac{1}{2}\rangle = 0\ . \qquad \text{(B.10c)}$$

In the above equations the constants g_{VS} and g_{AS} are defined as in Eq. (A. 2) while the integrals $I_{0,2,3}$ are given by

$$I_0 = \exp\left[-\frac{1}{6}\left(\frac{k^*}{\delta}\right)^2\right],$$
$$I_2 = \frac{-i}{3^{\frac{1}{2}}}\frac{k^*}{\delta} I_0, \qquad I_3 = \frac{-i}{3^{\frac{1}{2}}}\delta I_0. \tag{B.11}$$

The resonance production cross sections are obtained from the matrix element of Eq. (B.10) via the expression

$$\frac{d\sigma(E, E\,t)}{dt} = \text{CONST} \times \frac{M_B}{E^2}\left\{\sum_S |\langle B\ S|\mathcal{M}|p\ S=\tfrac{1}{2}\rangle|^2 + \left[g_{A3}^- - g_{A3}',\ g_{AS}^- - g_{AS}',\ W_{\pm} - W_{\mp}\right]\right\}, \tag{B.12}$$

$$B = D_{13},\ S_{11},\ P_{33},$$

with the second term in the curly brackets giving the contribution from $S = -\frac{1}{2}$ initial proton states. For incident antineutrinos, the sign of the axial-vector amplitudes is reversed, while for neutron targets, the sign of the isovector amplitudes is reversed.

In our numerical calculations we have followed Abdullah and Close[10] in choosing

$$\delta^2 = 0.14\ (\text{GeV})^2, \tag{B.13}$$
$$M_q = 0.333\ \text{GeV}.$$

The "no mixing" case[28] is of course evaluated with $\theta_D = \theta_S = 0$, while when we include mixing we use the angles suggested by Hey, Litchfield and Cashmore,[19]

$$\theta_D = 10.2^\circ, \quad \theta_S = -29.4^\circ \ . \tag{B.14}$$

In an earlier paper, Faiman and Hendry[29] suggested the mixing angles $\theta_D \approx 35^\circ$ or 127°, $\theta_S \approx -35^\circ$ or -90°. These all give results qualitatively similar to those found using Eq. (B.14), except for the case $\theta_S = 90^\circ$. Here we find $r_n^{BNL}(\nu S_{11}^+; \theta_W) \equiv 1$, as a result of the vanishing[30] of the electromagnetic transition $\gamma + p \to S_{11}^+(8^{3/2})$. However, as Faiman and Hendry[29] in fact argued, the fact that the $S_{11}(1505)$ is electromagnetically excited argues against the choice of 90° for the mixing angles θ_S.

APPENDIX C

We give in this appendix details of the resonance production calculation using the MIT bag model.[11] Although internal quark motions are treated relativistically in this model, in the approximation which we use the overall resonance center of mass is treated as static; hence again an ad hoc choice of frame is necessary. For calculational convenience, we have chosen to work in the Breit frame, allowing us to take over intact the lepton kinematics developed in Appendix B.

We begin by constructing the bag model wave functions for the p, P_{33}, D_{13} and S_{11}. In the case of the D_{13} there is only one possible bag model wave function, and hence no mixing, but for the S_{11} there are two possible wave functions, which we denote by $S_{11}(1), S_{11}(2)$. We define the physical $S_{11}(1505)$ state by again introducing a mixing angle θ_S^B (not necessarily the same as the mixing angle θ_S of the nonrelativistic quark model),

$$S_{11}(1505) = \cos\theta_S^B\, S_{11}(1) - \sin\theta_S^B\, S_{11}(2). \tag{C.1}$$

For the wave functions of states with angular momentum component S, we have

$$\psi[p(938);\tfrac{1}{2}S] = \psi_S^O(sss)\ \frac{1}{2^{\frac{1}{2}}}[|\tfrac{1}{2}S>_\alpha \psi_\alpha(\mathcal{PPN}) + |\tfrac{1}{2}S>_\beta \psi_\beta(\mathcal{PPN})]\ , \tag{C.2}$$

$$\psi[P_{33}^+(1232);\tfrac{3}{2}S] = \psi_S^O(sss)\ |\tfrac{3}{2}S>_S\ \psi_S(\mathcal{PPN})\ .$$

$$\psi[D_{13}^+(1505);\tfrac{3}{2}S] = |\tfrac{3}{2}S>_S \frac{1}{2^{\frac{1}{2}}}[\psi_\alpha^O(ssp)\ \psi_\alpha(\mathcal{PPN}) + \psi_\beta^O(ssp)\ \psi_\beta(\mathcal{PPN})]\ ,$$

$$\psi[S_{11}(1);\tfrac{1}{2}S] = \tfrac{1}{2}\,\psi_\alpha^O(ssp)\,[-|\tfrac{1}{2}S>_\alpha \psi_\alpha(\mathcal{PPN}) + |\tfrac{1}{2}S>_\beta \psi_\beta(\mathcal{PPN})]$$

$$+\tfrac{1}{2}\,\psi_\beta^O(ssp)\,[|\tfrac{1}{2}S>_\alpha \psi_\beta(\mathcal{PPN}) + |\tfrac{1}{2}S>_\beta \psi_\alpha(\mathcal{PPN})]\ ,$$

$$\psi[S_{11}(2);\tfrac{1}{2}S] = \psi_S^O(ssp)\ \frac{1}{2^{\frac{1}{2}}}[|\tfrac{1}{2}S>_\alpha \psi_\alpha(\mathcal{PPN}) + |\tfrac{1}{2}S>_\beta \psi_\beta(\mathcal{PPN})]\ .$$

The spin and SU_3 wave functions are precisely as in Eq. (B.6), while the orbital wave functions are constructed in terms of quark Dirac s- and p- orbitals in the following manner,

$$\psi_S^O(sss) = \psi_{s_0}(r_1)\psi_{s_0}(r_2)\psi_{s_0}(r_3),$$

$$\psi_S^O(ssp) = \frac{1}{3^{\frac{1}{2}}}[\psi_{s_1}(r_1)\psi_{s_1}(r_2)\psi_p(r_3) + \psi_{s_1}(r_1)\psi_p(r_2)\psi_{s_1}(r_3)$$

$$+ \psi_p(r_1)\psi_{s_1}(r_2)\psi_{s_1}(r_3)], \qquad (C.3)$$

$$\psi_\alpha^O(ssp) = \frac{1}{6^{\frac{1}{2}}}[\psi_p(r_1)\psi_{s_1}(r_2)\psi_{s_1}(r_3)+\psi_{s_1}(r_1)\psi_p(r_2)\psi_{s_1}(r_3)$$

$$-2\psi_{s_1}(r_1)\psi_{s_1}(r_2)\psi_p(r_3)],$$

$$\psi_\beta^O(ssp) = \frac{1}{2^{\frac{1}{2}}}[\psi_p(r_1)\psi_{s_1}(r_2)\psi_{s_1}(r_3)-\psi_{s_1}(r_1)\psi_p(r_2)\psi_{s_1}(r_3)].$$

The Dirac orbitals are given in turn by

$$\psi_{s_0}(r) = \frac{N_{s_0}}{(4\pi)^{\frac{1}{2}}}\begin{pmatrix} ij_0(br) \\ -j_1(br)\vec{\sigma}\cdot\hat{r} \end{pmatrix}, \quad \psi_{s_1}(r) = \frac{N_{s_1}}{(4\pi)^{\frac{1}{2}}}\begin{pmatrix} ij_0(b_1 r) \\ -j_1(b_1 r)\vec{\sigma}\cdot\hat{r} \end{pmatrix}, \qquad (C.4)$$

$$\psi_p(r) = \frac{N_p}{(4\pi)^{\frac{1}{2}}}\begin{pmatrix} ij_1(ar)\vec{\sigma}\cdot\hat{r} \\ j_0(ar) \end{pmatrix};$$

note that these are matrices in Pauli spin space which act on the spin wave functions of Eq. (C.2). The functions j_0 and j_1 are the usual vector spherical harmonics defined below in Eq. (C.11) while the constants a, b and b_1 are defined by

$$a = \frac{\omega_{11}}{R_1}, \quad b = \frac{\omega_{1-1}}{R_0}, \quad b_1 = \frac{\omega_{1-1}}{R_1}, \quad \omega_{1-1} = 2.04, \quad \omega_{11} = 3.81, \qquad (C.5)$$

with R_0 and R_1 the bag radii appropriate to the sss and ssp orbitals respectively. Following the MIT group,[11] we use the value

$$R_0 = 0.97\, M_\pi^{-1} \quad . \tag{C.6}$$

The relation between R_1 and R_0 is fixed by the equation[31]

$$\left(\frac{R_1}{R_0}\right)^4 = \frac{2\omega_{1-1} + \omega_{11}}{3\omega_{1-1}} \quad , \tag{C.7}$$

giving

$$R_1 = 1.07\, R_0 \quad . \tag{C.7}$$

while the normalization constants N_s and N_p are given by

$$N_{s_0} = \left[\frac{\omega_{1-1}^3}{2R_0^3(\omega_{1-1}-1)\sin^2\omega_{1-1}}\right]^{\frac{1}{2}}, \quad N_{s_1} = \left[\frac{\omega_{1-1}^3}{2R_1^3(\omega_{1-1}-1)\sin^2\omega_{1-1}}\right]^{\frac{1}{2}} ,$$

$$N_p = \left[\frac{\omega_{11}^3}{2R_1^3(\omega_{11}+1)\sin^2\omega_{11}}\right]^{\frac{1}{2}} . \tag{C.8}$$

Having specified the bag model wave functions, we proceed to evaluate matrix elements of the interaction operator $\mathcal{H}'$ defined in Eq. (B.8). Again it suffices to keep only one quark contribution and to multiply at the end by a factor of 3. Since nonvanishing contributions to the matrix elements for D_{13} or S_{11} excitation from a nucleon are obtained only when the current couples to the single p orbital in the D_{13} or S_{11} wave functions, we define an effective interaction operator $\mathcal{H}'_{ps}$ in spin-unitary spin space as the matrix element of Eq. (B.8) taken from an s_0 to a p Dirac orbital. Evaluation of the spatial integrals then gives

$$\mathcal{H}'_{ps} = \frac{3i}{2}\sum_{j=0,3,8} g_{Vj}\lambda_j \{ -I_1 W_0 \sigma_z - [I_2 + \tfrac{2}{3}(I_3 - 2I_4)] W_z \sigma_z$$
$$- 2^{\frac{1}{2}}[I_2 + \tfrac{2}{3}(I_3 + I_4)](W_+\sigma_- + W_-\sigma_+)\}$$
$$- \frac{3i}{2}\sum_j g_{Aj}\lambda_j \{(I_2 + 2I_3)W_0 + I_1 W_z + 2^{\frac{1}{2}} I_5 (W_+\sigma_- - W_-\sigma_+)\} \quad , \tag{C.9}$$

with the components of $\vec{W}$ as defined in Eq. (B. 9) and with the integrals $I_{1,\ldots,5}$ given by

$$I_1 = N_{s_0} N_p \int_0^{R_0} r^2 dr\, j_1(k^* r)[j_0(ar)j_1(br) - j_1(ar)j_0(br)] ,$$

$$I_2 = N_{s_0} N_p \int_0^{R_0} r^2 dr\, j_0(k^* r)[j_0(ar)j_0(br) - j_1(ar)j_1(br)] ,$$

$$I_3 = N_{s_0} N_p \int_0^{R_0} r^2 dr\, j_0(k^* r)[j_1(ar)j_1(br)] ,$$

$$I_4 = N_{s_0} N_p \int_0^{R_0} r^2 dr\, j_2(k^* r)[j_1(ar)j_1(br)] ,$$

$$I_5 = N_{s_0} N_p \int_0^{R_0} r^2 dr\, j_1(k^* r)[j_0(ar)j_1(br) + j_1(ar)j_0(br)] . \qquad \text{(C. 10)}$$

The spherical Bessel functions $j_{0,1,2}$ are, as usual, given by

$$j_0(x) = \frac{\sin x}{x} ,$$

$$j_1(x) = \frac{\sin x}{x^2} - \frac{\cos x}{x} , \qquad \text{(C. 11)}$$

$$j_2(x) = (\frac{3}{x^3} - \frac{1}{x}) \sin x - \frac{3 \cos x}{x^2} .$$

Because the s_1-orbitals in the D_{13} and S_{11} have a radius R_1 which is slightly different from the radius R_0 of the s_0 orbitals in the nucleon, their overlap differs slightly from unity, giving

$$1-\delta \equiv N_{s_0} N_{s_1} \int_0^{R_0} r^2 dr[\, j_0(b_1 r) j_0(br) + j_1(b_1 r) j_1(br)] . \qquad \text{(C. 12)}$$

However, since in this paper we only study ratios characterizing different modes of excitation of the same resonance, the overlap factor defined in Eq. (C. 12) always divides out. Proceeding to evaluate the spin-unitary spin matrix elements of $\mathcal{M}_{ps}$ (again taking the lepton momentum transfer $\vec{k}^*$ to lie along the z axis and quantizing spins along this direction), we find the following production matrix elements,

$$< D_{13}, S = \frac{3}{2} | \mathcal{H} | p, S = \tfrac{1}{2} >$$

$$= \frac{i}{2} (1-\delta)^2 2^{\frac{1}{2}} W_- \{ -[I_2 + \tfrac{2}{3}(I_3+I_4)](g_{VS} - \tfrac{1}{3} g_{V3}) + I_5 (g_{AS} - \tfrac{1}{3} g_{A3}) \} ,$$

$$< D_{13}, S = \tfrac{1}{2} | \mathcal{H} | p, S = \tfrac{1}{2} >$$

$$= \frac{i}{3^{\frac{1}{2}}} (1-\delta)^2 \{ I_1 W_0 + [I_2 + \tfrac{2}{3}(I_3 - 2I_4)] W_z \} (g_{VS} - \tfrac{1}{3} g_{V3}) ,$$

$$< D_{13}, S = -\tfrac{1}{2} | \mathcal{H} | p, S = \tfrac{1}{2} >$$

$$= \frac{i}{6^{\frac{1}{2}}} (1-\delta)^2 W_+ \{ [I_2 + \tfrac{2}{3}(I_3+I_4)] (g_{VS} - \tfrac{1}{3} g_{V3}) + I_5 (g_{AS} - \tfrac{1}{3} g_{A3}) \} ,$$

$$< D_{13}, S = -\tfrac{3}{2} | \mathcal{H} | p, S = \tfrac{1}{2} > = 0 \ ;$$

$$< S_{11}, S = \tfrac{1}{2} | \mathcal{H} | p, S = \tfrac{1}{2} >$$

$$= \frac{i}{3^{\frac{1}{2}}} (1-\delta)^2 \{ [(I_2 + 2I_3) W_0 + I_1 W_z] [\cos \theta_S^B g_{A3} + \tfrac{1}{2} \sin \theta_S^B (3 g_{AS} + g_{A3})]$$

$$+ [I_1 W_0 + (I_2 + \tfrac{2}{3} I_3 - \tfrac{4}{3} I_4) W_z] [\cos \theta_S^B (g_{VS} + \tfrac{2}{3} g_{V3}) + \tfrac{1}{2} \sin \theta_S^B (g_{VS} + \tfrac{5}{3} g_{V3})] \},$$

$$< S_{11}, S = -\tfrac{1}{2} | \mathcal{H} | p, S = \tfrac{1}{2} >$$

$$= \frac{i}{3^{\frac{1}{2}}} (1-\delta)^2 2^{\frac{1}{2}} W_+ \{ [I_2 + \tfrac{2}{3}(I_3+I_4)] [\cos \theta_S^B (g_{VS} + \tfrac{2}{3} g_{V3}) + \tfrac{1}{2} \sin \theta_S^B (g_{VS} + \tfrac{5}{3} g_{V3})]$$

$$+ I_5 [\cos \theta_S^B (g_{AS} + \tfrac{2}{3} g_{A3}) + \tfrac{1}{2} \sin \theta_S^B (g_{AS} + \tfrac{5}{3} g_{A3})] \} \quad . \qquad \text{(C.1}$$

To calculate matrix elements for the p to P_{33} transition, we follow a precisely analogous procedure. We first define an effective interaction operator $\mathcal{H}_{ss}$ in spin-unitary spin space as the matrix element of Eq. (B.8) taken from an s_0 to an s_0 Dirac orbital. Evaluation of the spatial integrals then gives

$$\mathcal{H}_{ss} = \frac{3}{2} \sum_{j=0,3,8} g_{Vj} \lambda_j \{ \hat{I}_1 W_0 + 2^{3/2} \hat{I}_2 (\sigma_- W_+ - \sigma_+ W_-) \}$$

$$+ \frac{3}{2} \sum_{j=0,3,8} g_{Aj} \lambda_j \{ (\hat{I}_1 + \tfrac{2}{3} \hat{I}_3) \sigma W_z + 2^{\frac{1}{2}} (\hat{I}_1 + \tfrac{2}{3} \hat{I}_4) (\sigma_+ W_- + \sigma_- W_+) \} \quad . \qquad \text{(C.1}$$

with the integrals $\hat{I}_{1,\ldots,4}$ given by

$$\hat{I}_1 = N_{s_0}^2 \int_0^{R_0} r^2 dr [\, j_0^2(br) - j_1^2(br)\,]\, j_0(k^* r)\ ,$$

$$\hat{I}_2 = N_{s_0}^2 \int_0^{R_0} r^2 dr\, j_0(br) j_1(br) j_1(k^* r)\ ,$$

$$\hat{I}_3 = N_{s_0}^2 \int_0^{R_0} r^2 dr\, j_1^2(br)[\, j_0(k^* r) - 2 j_2(k^* r)\,]\ .$$

$$\hat{I}_4 = N_{s_0}^2 \int_0^{R_0} r^2 dr\, j_1^2(br)[\, j_0(k^* r) + j_2(k^* r)\,]\ . \qquad \text{(C.15)}$$

Evaluating the spin-unitary spin matrix elements then gives

$$\langle P_{33}, S=\tfrac{3}{2} | \mathcal{H} | p, S=\tfrac{1}{2} \rangle = \frac{-2W}{3^{\frac{1}{2}}} [\, -2\, \hat{I}_2 g_{V3} + (\hat{I}_1 + \tfrac{2}{3}\hat{I}_4) g_{A3}\,]\ ,$$

$$\langle P_{33}, S=\tfrac{1}{2} | \mathcal{H} | p, S=\tfrac{1}{2} \rangle = \frac{2^{3/2}}{3} W_z (\hat{I}_1 + \tfrac{2}{3}\hat{I}_3) g_{A3}\ ,$$

$$\langle P_{33}, S=-\tfrac{1}{2} | \mathcal{H} | p, S=\tfrac{1}{2} \rangle = \frac{2}{3} W_+ [\, 2\, \hat{I}_2\, g_{V3} + (\hat{I}_1 + \tfrac{2}{3}\hat{I}_4) g_{A3}\,]\ ,$$

$$\langle P_{33}, S=-\tfrac{3}{2} | \mathcal{H} | p, S=\tfrac{1}{2} \rangle = 0\ . \qquad \text{(C.16)}$$

The resonance production cross sections are obtained from the matrix elements of Eqs. (C.13) and (C.16) by substitution into Eq. (B.12).

Unlike the situation in the nonrelativistic quark model, where phenomenological determinations of the mixing angles have been made, there is at present no clear theoretical guide as to what value should be assigned to the bag model S_{11} mixing angle θ_S^B. Hence, we have done the numerical work in the bag case for a sequence of mixing angles spanning[32] the range from $-\frac{\pi}{2}$ to $\frac{\pi}{2}$, with results for the ratios r_n^{BNL} and R_n^{BNL}/R_{ch}^{BNL} as summarized in Table VII. We see that qualitatively similar results are obtained for

all angles except those in the vicinity of -30° to -45°. At $\theta_S^B = -45^\circ$, the ratio $r_n^{BNL}(\nu\, S_{11}^+ : 0_W)$ is identically equal to 1, indicating that the transition $\gamma + p \to S_{11}^+(1505)$ is forbidden at $\theta_S^B = -45^\circ$. [Indeed, as expected, $r_{va/em}(\nu\, S_{11}^+)$ becomes infinite in the bag model at $\theta_S^B = -45^\circ$] . Since, as argued at the end of Appendix B, electromagnetic excitation of the S_{11} is observed, angles θ_S^B near -45° would seem to be an unlikely choice for the bag model mixing angle. It is tempting, although very conjectural, to carry the reasoning one step further, by identifying the wave function of Eq. (C.1) with $\theta_S^B = -45^\circ$ as a bag model analog of the $\pm\, S_{11}(8^{3/2})$ quark model state (for which $\gamma + p \to S_{11}^+$ also vanishes[33]), and the orthogonal state, obtained from Eq. (C.1) with $\theta_S^B = 45^\circ$, as a bag model analog of the $S_{11}(8^{\frac{1}{2}})$ state. If this analogy makes sense,[34] then the quark model wave function with $\theta_S \approx -30^\circ$ would have as its bag model analog the state described by Eq. (C.1) with either $\theta_S^B = 45^\circ - 30^\circ = 15^\circ$ or $\theta_S^B = 45^\circ + 30^\circ = 75^\circ$, giving behavior very close to that found for $\theta_S^B = 0^\circ$ or $\theta_S^B = 90^\circ$ respectively. In Tables IIB through VI, we have given results obtained from the bag model calculation for $\theta_S^B = 0^\circ$, $\theta_S^B = 90^\circ$, which look very similar and give ratios R_n^{BNL}/R_{ch}^{BNL} of around 1/4, and also for $\theta_S^B = -30^\circ$, which as has already been stressed, behaves in a qualitatively different fashion and gives ratios R_n^{BNL}/R_{ch}^{BNL} in the neighborhood of $\frac{1}{2}$.

APPENDIX D

In this appendix we briefly discuss the charge exchange corrections needed to apply the results of the text (which were derived assuming free nucleon targets) to the case of resonance production on a complex nuclear target.[35] We start from the second relation in Eq. (10) which, using the definitions of Eq. (5), can be rewritten in the form,

$$\frac{1}{4}\ \frac{r_n^{BNL}(\nu B^{+,0};\theta_W)}{r_n^{BNL}(\nu P_{33}^{+,0};\theta_W)} = \frac{R_n^{BNL}(\nu B^{+,0}/P_{33}^{+,0})}{R_{ch}^{BNL}(\nu B^{+}/P_{33}^{+})} \tag{D.1}$$

$$= \left[\frac{\sigma_n^{BNL}(\nu B^{+}) + \sigma_n^{BNL}(\nu B^{0})}{2\,\sigma_{ch}^{BNL}(\nu B^{+})}\right]\left[\frac{\sigma_n^{BNL}(\nu P_{33}^{+}) + \sigma_n^{BNL}(\nu P_{33}^{0})}{2\sigma_{ch}^{BNL}(\nu P_{33}^{+})}\right]^{-1},$$

$$B = D_{13} \text{ or } S_{11}.$$

Following the reasoning of Eqs. (6) - (10), we obtain for the two square bracketed quantities on the right-hand side of Eq. (D.1) the individual predictions (in the Weinberg-Salam model)

$$R_{n/ch}^{BNL}(\nu B^{+,0}) \equiv \frac{\sigma_n^{BNL}(\nu B^{+}) + \sigma_n^{BNL}(\nu B^{0})}{2\,\sigma_{ch}^{BNL}(\nu B^{+})} = \frac{1}{4}\, r_n^{BNL}(\nu B^{+,0};\theta_W), \tag{D.2}$$

$$R_{n/ch}^{BNL}(\nu P_{33}^{+,0}) \equiv \frac{\sigma_n^{BNL}(\nu P_{33}^{+}) + \sigma_n^{BNL}(\nu P_{33}^{0})}{2\,\sigma_{ch}^{BNL}(\nu P_{33}^{+})} = r_n^{BNL}(\nu P_{33}^{+,0};\theta_W).$$

The ratios on the left of Eq. (D.2) still refer to resonance production on free nucleon targets. To extract these ratios from experiments on complex nuclear targets, nuclear charge exchange corrections are needed. For simplicity, we consider the case of an isotopically neutral target T, containing equal numbers of protons and neutrons. We define the observable ratios

(D.3)

$$R'^{BNL}_{n/ch}(\nu T \to B \to N\pi^0) = \frac{\sigma_n^{BNL}(\nu T \to \nu B^+ \ldots \to \nu N\pi^0 \ldots) + \sigma_n^{BNL}(\nu T \to \nu B^0 \ldots \to \nu N\pi^0 \ldots)}{2\sigma_{ch}^{BNL}(\nu T \to \mu^- B^+ \ldots \to \mu^- N\pi^0 \ldots)},$$

$$R'^{BNL}_{n/ch}(\nu T \to B \to N\eta) = \frac{\sigma_n^{BNL}(\nu T \to \nu B^+ \ldots \to \nu N\eta \ldots) + \sigma_n^{BNL}(\nu T \to \nu B^0 \ldots \to \nu N\eta \ldots)}{2\,\sigma_{ch}^{BNL}(\nu T \to \mu^- B^+ \ldots \to \mu^- N\eta \ldots)},$$

and (D.4)

$$R'^{BNL}_{n/ch}(\nu T \to P_{33} \to N\pi^0) = \frac{\sigma_n^{BNL}(\nu T \to \nu P_{33}^+ \ldots \to \nu N\pi^0 \ldots) + \sigma_n^{BNL}(\nu T \to \nu P_{33}^0 \ldots \to \nu N\pi^0 \ldots)}{2\left[\sigma_{ch}^{BNL}(\nu T \to \mu^- P_{33}^+ \ldots \to \mu^- N\pi^0 \ldots) + \sigma_{ch}^{BNL}(\nu T \to \mu^- P_{33}^{++} \ldots \to \mu^- N\pi^0 \ldots)\right]},$$

where ... indicates unobserved nuclear fragments and where the final state π^0 or η is the emerging particle observed <u>after</u> the resonance decay products have had a chance to charge exchange in the target nucleus. As an immediate consequence of isospin invariance we find

$$\begin{aligned} \Gamma(B^0 \to n\pi^0) &= \Gamma(B^+ \to p\pi^0), \\ \Gamma(B^0 \to p\pi^-) &= \Gamma(B^+ \to n\pi^+), \\ \Gamma(B^0 \to n\eta) &= \Gamma(B^+ \to p\eta). \end{aligned} \qquad (D.5)$$

Since in an isotopically neutral target the $\pi^{+,-}$ have equal probabilities to charge exchange into a π^0 or to scatter inelastically into an η, we can immediately conclude that the effects of nuclear interactions in the numerator and denominator of Eq. (D. 3) are precisely the same. Thus for the $I = \frac{1}{2}$ resonances no charge exchange correction factor appears in relating Eqs. (D. 2) to Eq. (D. 3), and we have

$$R'^{BNL}_{n/ch}(\nu T \to D_{13} \to N\pi^0) = R^{BNL}_{n/ch}(\nu D_{13}^{+,0}), \tag{D. 6}$$

$$R'^{BNL}_{n/ch}(\nu T \to S_{11} \to N\eta) = R'^{BNL}_{n/ch}(\nu T \to S_{11} \to N\pi^0) = R^{BNL}_{n/ch}(\nu S_{11}^{+,0}).$$

An analogous argument cannot be applied to P_{33} production because of the strong P_{33}^{++} contribution to the denominator of Eq. (D. 4). Using in this case the averaged charge exchange formula given by Adler, Nussinov and Paschos[36], we find

$$R'^{BNL}_{n/ch}(\nu T \to P_{33} \to N\pi^0) \approx \frac{\tilde{d}\,\frac{1}{2} + 1 - 2\tilde{d}}{\tilde{d}\,5 + 1 - 2\tilde{d}}\, R^{BNL}_{n/ch}(\nu P_{33}^{+,0}), \tag{D. 7}$$

with $\tilde{d}$ a parameter characterizing the pion charge exchange properties of the target nucleus T and with $\frac{1}{2}$ and 5 respectively the charged pion to neutral pion ratios expected for P_{33} production by the weak neutral and weak charged currents.[37] For an aluminum target we have $\tilde{d} \approx 0.16$, which when substituted

into Eq. (D.7) gives[37]

$$R'^{BNL}_{n/ch}(\nu\, Al \to P_{33} \to N\pi^0) \approx 0.51\, R^{BNL}_{n/ch}(\nu\, P^{+,0}_{33}) \,. \qquad (D.8)$$

Combining Eqs. (D.1), (D.6) and (D.3), we can restate the conclusion of Sec. 4 as follows for the case of an aluminum (or other light to medium weight[38] nuclear) target. In the Weinberg-Salam model, with $\sin^2 \theta_W$ in the range of experimental interest, the three models all predict that the ratios D_{13}/P_{33} and S_{11}/P_{33} observed on nuclear targets are smaller in the neutral current than in the charged current case. Hence if the $I = \frac{1}{2}$ resonances are found not to distort seriously invariant mass plots in the charged current case, they should not be expected to do so in the neutral current case. Also, the production of η's from the S_{11} relative to the P_{33} should be smaller in the neutral current than in the charged current case, with the ratio of resonant η production in the neutral current to that in the charged current given by Eqs. (D.2) and (D.6) and Tables IIB and VII.

REFERENCES

1. S. L. Adler, Ann. Phys. 50, 189 (1968).

2. S. L. Adler, Phys. Rev. D9, 229 (1974); S. L. Adler, S. Nussinov and E. A. Paschos, Phys. Rev. D9, 2125 (1974); S. L. Adler, IAS preprint; S. L. Adler, E. W. Colglazier, Jr., J. B. Healy, I. Karliner, J. Lieberman, Y. J. Ng and H.-S. Tsao, IAS preprints.

3. See for example, unpublished reports presented at the Argonne Symposium on Neutral Currents, March 6, 1975.

4. As discussed below, in electroproduction experiments there is virtually no excitation of the Roper resonance $P_{11}(1434)$, and so we ignore this state in our detailed weak production calculations. See also Ref. 16 below.

5. This point was emphasized to us by Prof. B. W. Lee.

6. This issue was raised in conversations with Prof. W. Y. Lee. See J.-C. Alder et. al., DESY 74/61, who observe η's from the $S_{11}(1505)$ in electroproduction.

7. In particular, the ratio $S_{11}(1505)/D_{13}(1514)$ is predicted to be $\sim 0.5 - 1.5$ in electroproduction, whereas the η studies of Ref. 6 show it to be around 0.25. Compare, for example the theoretical calculations of F. Ravndal, Phys. Rev. D5, 2849 (1972), D. Faiman and A. W. Hendry, Phys. Rev. 180, 1572 (1969) and T. Abdullah and F. E. Close, Phys. Rev. D5, 2332 (1972) with the experimental numbers given in Table I below.

8. In particular, all sign relations coming from applications of the Melosh transformation agree with experiment, and the Melosh

relations are mostly satisfied by the relativistic quark model of R. P. Feynman, M. Kislinger and F. Ravndal, Phys. Rev. D3. 2706 (1971) and F. Ravndal, Ref. 7, which in turn gives predictions quite similar to those of the nonrelativistic quark model employed below. For a discussion of the Melosh transformation and its relation to quark models see F. J. Gilman, SLAC-Pub-1532 (1975).

9. J. Walecka and P. A. Zucker, Phys. Rev. 167, 1479 (1968).

10. D. Faiman and A. W. Hendry, Phys. Rev. 173, 1720 (1968) and Phys. Rev. 180, 1572 (1969); T. Abdullah and F. E. Close, Phys. Rev. D5, 2332 (1972).

11. A. Chodos et. al., Phys. Rev. D9, 3471 (1974) and Phys. Rev. D10, 2599 (1974); J. F. Donoghue, E. Golowich and B. R. Holstein, Univ. of Mass. preprint.

12. S. Weinberg, Phys. Rev. Letters 19, 1264 (1967); A. Salam, in Elementary Particle Physics, edited by N. Svartholm (Almquist and Forlag, Stockholm, 1968), p. 367; S. Weinberg, Phys. Rev. D5, 1412 (1972). We ignore possible isoscalar strangeness and charm current pieces in the neutral current, which should couple very weakly to low-lying non-strange baryons.

13. We follow the metric conventions of J. D. Bjorken and S. D. Drell, Relativistic Quantum Fields (McGraw-Hill, New York, 1965, Appendix A).

14. We use BNL flux tables supplied by W. Y. Lee and L. Litt (private communication).

15. R. C. E. Devenish and D. H. Lyth, DESY 75/04 (1975).

16. If the weak matrix element for exciting the P_{11} state is appreciable, then the near absence of the electromagnetic transition implies that the ratio $r_n^{BNL}(\nu\, P_{11}^+; \theta_W)$, defined in analogy with Eq. (8), will be approximately 1, independent of θ_W. Hence from the numerical results of Table IIC we see that $R_n^{BNL}(\nu\, P_{11}^+/P_{33}^+)/R_{ch}^{BNL}(\nu\, P_{11}^+/P_{33}^+)$ will be of order $1/4 \times (1/0.4) \approx 0.6$ at most, for Weinberg angles in the range of interest, and so the conclusions reached in Sec. IV will apply to P_{11} production also.

17. A. B. Clegg, in Proceedings of the 6th International Symposium on Electron and Photon Interactions at High Energies, H. Rollnik and W. Pfeil, eds. (North Holland, 1974), p. 49.

18. We also include corrections to the Born approximation which bring it into agreement with soft pion predictions when the pion four momentum is zero--see Eq. (A.4).

19. A. J. G. Hey, P. J. Litchfield and R. J. Cashmore, CERN/D. Ph II/PHYS 74-19.

20. Since the D_{13} is in fact strongly electroproduced from protons, it appears that the bag model wave function for this state is not very satisfactory. The process $\gamma+p \to D_{13}(8^{3/2})$ in the quark model is also forbidden. In this sense, it is tempting to identify the bag model D_{13} wave function with the quark model $8^{3/2}$ state.

21. The metric conventions in this Appendix are thus opposite to those

of the remainder of the paper. In treating P_{33} excitation, apart from the inclusion of the ω exchange contribution we follow the approximations of Ref. 1 (neglect of $E_{1+}^{(3/2)}$, $L_{1+}^{(3/2)}$, $M_{1+}^{(3/2)}$ and π exchange contributions, all of which are very small or are suppressed, rather than enhanced, by unitarization).

22. This is just the customary assumption that bosons have monopole, rather than dipole, electromagnetic form factors. Numerical results are insensitive to the precise value of the scale mass, although our choice of 0.9 GeV is quite reasonable based on known charge radii.

23. See Sec. 5A of Ref. 1.

24. For a discussion of the magnitude of g_A^S, see S. L. Adler, IAS preprint.

25. H. Pilkuhn et. al., Nucl. Phys. B65, 460 (1973).

26. F. J. Gilman, Phys. Rev. 167, 1365 (1968).

27. This value is in reasonable agreement with the value $\beta = 2.7$ argued for on very different grounds by H. D. I. Abarbanel, C. G. Callan Jr. and D. H. Sharp, Phys. Rev. 143, 1225 (1966). The value of $\beta = -8$ preferred by Walecka and Zucker, Ref. 9, changes the sign of the dominant $M_{1+}^{(3/2)}$ photoproduction multipole and hence is unacceptable.

28. Abdullah and Close (Ref. 10) argue for the absence of mixing.

29. D. Faiman and A. W. Hendry, Phys. Rev. 173, 1720 (1968). We have changed the sign of θ_S quoted here because their phase convention is opposite to ours.

30. See the closely related discussion at the end of Appendix C.

31. Eq. (C.7a) is obtained from the bag model relations

$$4\pi B\, R_0^4 = 3\,\omega_{1-1}$$

$$4\pi B\, R_1^4 = 2\,\omega_{1-1} + \omega_{11}\ ,$$

with B the bag constant.

32. Resonance evaluation cross sections for $\theta_S^B + \pi$ are the same as for θ_S^B, so angles larger in magnitude than $\pi/2$ need not be considered.

33. R. G. Morehouse, Phys. Rev. Letters 16, 772 (1966).

34. This analogy does not carry over to other processes. For example, a comparison of the π decay of the S_{11} in the quark and bag models yields the relation $\theta_S^B \sim \theta_S$.

35. We wish to thank Prof. T. O'Halloran for raising the question of charge exchange corrections.

36. S. L. Adler, S. Nussinov and E. A. Paschos, Ref. 2, Eq. (24).

37. Eqs. (D.7) and (D.8) refer strictly to the purely resonant pion production component, with the nonresonant background subtracted away. When the nonresonant background is retained, the (charged pion)/(neutral pion) ratios are altered from their resonant values of 1/2 and 5, and the correction factor in aluminum becomes more like 0.6.

38. The parameter $\tilde{d}$ is a slowly varying function of atomic number A; see, for example, Table VII of S. L. Adler, S. Nussinov and E. A. Paschos, Ref. 2 and Table VIII of S. L. Adler, Ref. 2.

Resonance B	$I(J^P)$	Mass M_B (GeV)	Width Γ_B (GeV)
P_{33}	$3/2\ (3/2^+)$	1.232	0.114
P_{11}	$1/2\ (1/2^+)$	1.434	0.2
S_{11}	$1/2\ (1/2^-)$	1.505	0.1
D_{13}	$1/2\ (3/2^-)$	1.514	0.13

TABLE IA.

Low lying nucleon resonance parameters.

t $[(GeV)^2]$	$\sigma_T(D_{13}, t)$ (mb)	$\sigma_T(S_{11}, t)$ (mb)	$\sigma_T(P_{33}, t)$ (mb)
0	139	29.5	400
0.1	123	27.4	430
0.2	103	25.3	430
0.3	88	23.2	410
0.4	76	21.6	340
0.5	65	20.0	285
0.7	51	17.9	195
0.9	40	15.8	130
1.1	33	13.2	100
1.3	27	11.1	75
1.5	23	10.0	60
1.7	20	9.5	45
1.9	17	8.4	35

TABLE IB.

Ratio	$\sin^2\theta_W$	Born approx. model (without ω exchange)	Quark model (without mixing)	Bag model	Born approx. model (with ω exchange)	Quark model (with mixing)
$r_n^{BNL}(\nu D_{13}^{+}; \theta_W)$	0.1	0.84	0.70	1.00	0.79	0.70
	0.2	0.70	0.48	1.00	0.61	0.47
	0.3	0.58	0.31	1.00	0.46	0.31
	0.4	0.48	0.22	1.00	0.35	0.22
	0.5	0.40	0.19	1.00	0.27	0.20
$r_n^{BNL}(\nu D_{13}^{+,0}; \theta_W)$	0.1	0.69	0.78	0.81	0.68	0.78
	0.2	0.47	0.61	0.68	0.44	0.61
	0.3	0.33	0.48	0.61	0.28	0.48
	0.4	0.27	0.39	0.61	0.20	0.40
	0.5	0.30	0.36	0.66	0.20	0.36
$r_n^{BNL}(\bar{\nu} D_{13}^{+}; \theta_W)$	0.1	0.80	0.74	1.00	0.74	0.73
	0.2	0.63	0.61	1.00	0.53	0.60
	0.3	0.49	0.62	1.00	0.37	0.61
	0.4	0.39	0.76	1.00	0.26	0.76
	0.5	0.32	1.04	1.00	0.19	1.05
$r_n^{BNL}(\bar{\nu} D_{13}^{+,0}; \theta_W)$	0.1	0.63	0.76	0.83	0.63	0.76
	0.2	0.39	0.61	0.85	0.37	0.62
	0.3	0.29	0.56	1.05	0.23	0.56
	0.4	0.32	0.59	1.45	0.20	0.60
	0.5	0.48	0.72	2.03	0.29	0.73

TABLE IIA.

Table of ratios r_n^{BNL}, defined in Eq. (8) of the text, for $D_{13}(1514)$ production.

Ratio	$\sin^2\theta_W$	Born approx. model (without ω exchange)	Quark model (without mixing)	Bag model #1	Bag model #2	Born approx. model (with ω exchange)	Quark model (with mixing)	Bag model (#1, #2 mixture $\theta_S^B = -30^\circ$)
$r_n^{BNL}(\nu S_{11}^+; \theta_W)$	0.1	0.88	0.69	0.74	0.76	0.84	0.70	0.77
	0.2	0.78	0.45	0.53	0.57	0.71	0.46	0.62
	0.3	0.69	0.28	0.39	0.42	0.59	0.28	0.56
	0.4	0.61	0.18	0.31	0.31	0.49	0.17	0.59
	0.5	0.54	0.16	0.30	0.24	0.40	0.11	0.71
$r_n^{BNL}(\nu S_{11}^{+,0}; \theta_W)$	0.1	0.84	0.76	0.82	0.80	0.81	0.74	0.90
	0.2	0.71	0.56	0.68	0.63	0.65	0.53	0.84
	0.3	0.61	0.41	0.56	0.49	0.52	0.37	0.83
	0.4	0.53	0.30	0.49	0.39	0.43	0.25	0.87
	0.5	0.48	0.25	0.45	0.31	0.36	0.18	0.95
$r_n^{BNL}(\bar{\nu} S_{11}^+; \theta_W)$	0.1	0.91	0.65	0.79	0.77	0.86	0.62	0.90
	0.2	0.84	0.44	0.73	0.66	0.77	0.39	0.93
	0.3	0.80	0.38	0.83	0.68	0.72	0.30	1.11
	0.4	0.79	0.48	1.07	0.82	0.72	0.37	1.43
	0.5	0.80	0.72	1.47	1.09	0.77	0.59	1.89
$r_n^{BNL}(\bar{\nu} S_{11}^{+,0}; \theta_W)$	0.1	0.88	0.70	0.85	0.80	0.83	0.66	0.96
	0.2	0.82	0.51	0.79	0.69	0.73	0.44	0.99
	0.3	0.80	0.41	0.81	0.67	0.70	0.32	1.09
	0.4	0.83	0.42	0.91	0.74	0.75	0.32	1.27
	0.5	0.91	0.53	1.10	0.90	0.88	0.43	1.51

TABLE IIB.

Table of ratios r_n^{BNL}, defined in Eq. (8) of the text, for $S_{11}(1505)$ production.

Ratio	$\sin^2\theta_W$	Born approx. model (without ω exchange)	Quark model	Bag model	Born approx. model (with ω exchange)
$r_n^{BNL}(\nu P_{33}^+;\theta_W)$	0.1	0.83	0.83	0.83	0.79
$= r_n^{BNL}(\nu P_{33}^{+,0};\theta_W)$	0.2	0.69	0.68	0.69	0.62
	0.3	0.58	0.56	0.58	0.49
	0.4	0.49	0.46	0.49	0.38
	0.5	0.42	0.39	0.43	0.31
$r_n^{BNL}(\bar{\nu} P_{33}^+;\theta_W)$	0.1	0.87	0.87	0.86	0.79
$= r_n^{BNL}(\bar{\nu} P_{33}^{+,0};\theta_W)$	0.2	0.79	0.79	0.77	0.65
	0.3	0.77	0.78	0.73	0.58
	0.4	0.80	0.83	0.74	0.58
	0.5	0.38	0.93	0.80	0.66

TABLE IIC.

Table of ratios r_n^{BNL}, defined in Eq. (8) of the text, for $P_{33}(1232)$ production.

Ratio tabulated	Born approx. model (without ω exchange)	Quark model (without mixing)	Bag model	Born approx. model (with ω exchange)	Quark model (with mixing)	Bag model (#1, #2 mixture $\theta_S^B = -30^\circ$)
$r^{BNL}_{va/em}(\nu D^+_{13})$	4.0	1.2	∞ [a]	2.4	1.2	-
$r^{BNL}_{va/em}(\nu S^+_{11})$	6.1	1.1	#1: 1.3, #2: 1.8	4.3	1.3	0.90
$r^{BNL}_{va/em}(\nu P^+_{33})$	3.1	3.1	2.9	2.4	-	-

TABLE III.

Table of ratios $r^{BNL}_{va/em}(\nu B^+)$, defined in Eq. (11) of the text.

[a] An infinite ratio is obtained here because $\gamma + p \rightarrow D^+_{13}$ is forbidden in the bag model. See the discussion in the text.

Ratio tabulated	Born approx. model (without ω exchange)	Quark model (without mixing)	Bag model	Born approx. model (with ω exchange)	Quark model (with mixing)	Bag model (#1, #2 mixture $\theta_S^B = -30^\circ$)
$r^{BNL}_{ch\ \bar{\nu}/\nu}(D_{13})$	0.61	0.50	0.33	0.71	0.49	-
$r^{BNL}_{ch\ \bar{\nu}/\nu}(S_{11})$	0.53	0.47	#1: 0.40, #2: 0.34	0.41	0.41	0.63
$r^{BNL}_{ch\ \bar{\nu}/\nu}(P_{33})$	0.48	0.42	0.54	0.48	-	-

TABLE IV.

Table of ratios $r^{BNL}_{ch\ \bar{\nu}/\nu}(B)$, defined in Eq. (11) of the text.

FIGURE CAPTION

Figure 1. Born approximation diagrams, including ω exchange, for the process $\gamma + N \rightarrow \pi + N$.

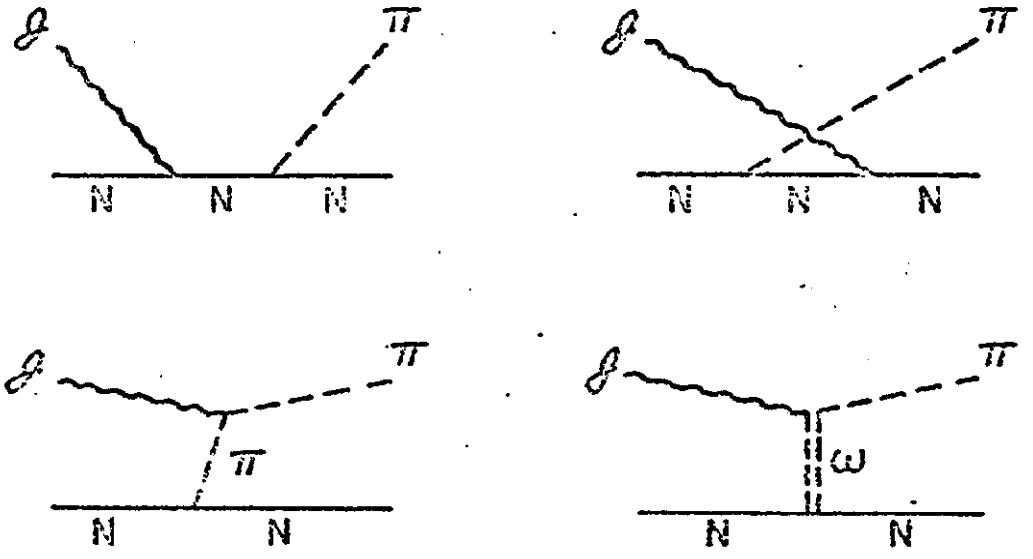

FIGURE 1.

Ratio tabulated	$\sin^2\theta_W$	Born approx. model (without ω exchange)	Quark model (without mixing)	Bag model		Born approx. model (with ω exchange)	Quark model (with mixing)	Bag mo (#1, #2 mi
$\frac{R_n^{BNL}(\nu D_{13}^+/P_{33}^+)}{R_{ch}^{BNL}(\nu D_{13}^+/P_{33}^+)}$	0.1	0.25	0.21	0.30		0.25	0.21	-
	0.2	0.25	0.18	0.36		0.25	0.17	-
	0.3	0.25	0.14	0.43		0.23	0.14	-
	0.4	0.24	0.12	0.51		0.23	0.12	-
	0.5	0.24	0.12	0.58		0.22	0.13	-
$\frac{R_n^{BNL}(\nu D_{13}^{+,0}/P_{33}^{+,0})}{R_{ch}^{BNL}(\nu D_{13}^+/P_{33}^+)}$	0.1	0.20	0.23	0.24		0.22	0.23	-
	0.2	0.15	0.22	0.25		0.17	0.22	-
	0.3	0.11	0.21	0.26		0.12	0.21	-
	0.4	0.08	0.21	0.31		0.09	0.22	-
	0.5	0.09	0.23	0.38		0.08	0.23	-
				#1	#2			
$\frac{R_n^{BNL}(\nu S_{11}^+/P_{33}^+)}{R_{ch}^{BNL}(\nu S_{11}^+/P_{33}^+)}$	0.1	0.27	0.21	0.22	0.23	0.27	0.21	0.23
	0.2	0.28	0.17	0.19	0.21	0.29	0.17	0.22
	0.3	0.30	0.13	0.17	0.18	0.30	0.13	0.24
	0.4	0.31	0.10	0.16	0.16	0.32	0.09	0.30
	0.5	0.32	0.10	0.17	0.14	0.32	0.07	0.41
$\frac{R_n^{BNL}(\nu S_{11}^{+,0}/P_{33}^{+,0})}{R_{ch}^{BNL}(\nu S_{11}^+/P_{33}^+)}$	0.1	0.25	0.23	0.25	0.24	0.26	0.22	0.27
	0.2	0.26	0.21	0.25	0.23	0.25	0.19	0.30
	0.3	0.26	0.18	0.24	0.21	0.22	0.17	0.36
	0.4	0.27	0.16	0.25	0.20	0.19	0.14	0.44
	0.5	0.29	0.16	0.26	0.18	0.14	0.12	0.55

TABLE V.

Comparison of neutral current with charged current D_{13}/P_{33} and S_{11}/P_{33} ratios, as derived from Table II via Eq. (10) of the text.

Ratio tabulated	Born approx. model (without ω exchange)	Quark model (without mixing)	Bag model		Born approx. model (with ω exchange)	Quark model (with mixing)	Bag model (#1, #2 mixt $\theta_S^B = -30^\circ$
$\frac{R_{ch}^{BNL}(\nu D_{13}^+/P_{33}^+)}{R_{em}^{BNL}(D_{13}^+/P_{33}^+)}$	5.2	1.6	∞ [a]		4.0	1.6	-
			#1	#2			
$\frac{R_{ch}^{BNL}(\nu S_{11}^+/P_{33}^+)}{R_{em}^{BNL}(S_{11}^+/P_{33}^+)}$	7.9	1.4	1.8	2.5	7.2	1.7	1.2

TABLE VI.

Comparison of charged current with electroproduction D_{13}/P_{33} and S_{11}/P_{33} ratios, as derived from Table III via Eq. (12) of the text.

[a] An infinite ratio is obtained here because $\gamma + p \to D_{13}^+$ is forbidden in the bag model. See the discussion in the text.

Ratio	$\sin^2\theta_W$	Bag model S_{11} mixing angle θ_S^B: -60°	-45°	-30°	0° (#1)	30°	45°	60°	90° (#2)
$r_n^{BNL}(\nu S_{11}^+; \theta_W)$	0.1	0.81	1.0	0.77	0.74	0.74	0.75	0.75	0.76
	0.2	0.64	1.0	0.62	0.53	0.54	0.55	0.55	0.57
	0.3	0.50	1.0	0.56	0.39	0.39	0.40	0.40	0.42
	0.4	0.39	1.0	0.59	0.31	0.30	0.30	0.30	0.31
	0.5	0.30	1.0	0.71	0.30	0.26	0.25	0.25	0.24
$r_n^{BNL}(\nu S_{11}^{+,0}; \theta_W)$	0.1	0.80	0.87	0.90	0.82	0.81	0.81	0.80	0.80
	0.2	0.62	0.79	0.84	0.68	0.65	0.65	0.64	0.63
	0.3	0.48	0.74	0.83	0.56	0.53	0.52	0.51	0.49
	0.4	0.37	0.74	0.87	0.49	0.44	0.42	0.41	0.39
	0.5	0.28	0.78	0.95	0.45	0.38	0.36	0.34	0.31
$\frac{R_n^{BNL}(\nu S_{11}^+/P_{33}^+)}{R_{ch}^{BNL}(\nu S_{11}^+/P_{33}^+)}$	0.1	0.24	0.30	0.23	0.22	0.22	0.23	0.23	0.23
	0.2	0.23	0.36	0.22	0.19	0.20	0.20	0.20	0.21
	0.3	0.22	0.43	0.24	0.17	0.17	0.17	0.17	0.18
	0.4	0.20	0.51	0.30	0.16	0.15	0.15	0.15	0.16
	0.5	0.17	0.58	0.41	0.17	0.15	0.15	0.15	0.14
$\frac{R_n^{BNL}(\nu S_{11}^{+,0}/P_{33}^{+,0})}{R_{ch}^{BNL}(\nu S_{11}^+/P_{33}^+)}$	0.1	0.24	0.26	0.27	0.25	0.24	0.24	0.24	0.24
	0.2	0.22	0.29	0.30	0.25	0.24	0.24	0.23	0.23
	0.3	0.21	0.32	0.36	0.24	0.23	0.22	0.22	0.21
	0.4	0.19	0.38	0.44	0.25	0.22	0.21	0.21	0.20
	0.5	0.16	0.45	0.55	0.26	0.22	0.21	0.20	0.18

TABLE VII.

Ratios in Table IIB and Table VI vs. mixing angle θ_S^B for the two bag model S_{11} configurations. The wave functions labeled #1 and #2 correspond to $\theta_S^B = 0^\circ$, 90° respectively.